Resource-driven Design and Optimization of Hybrid Renewable Energy Systems for Namibia's off- Grid Communities

Ndemuhanga V. Nghuumbwa , T. Wanjekeche * , E. Hamatwi , M. Kanime

Posted Date: 13 March 2026

doi: 10.20944/preprints202603.1075.v1

Keywords: energy storage system; hybrid renewable energy system; optimization; renewable energy; rural area

 doi:10.20944/preprints202603.1075.v1

Article

Resource-driven Design and Optimization of Hybrid Renewable Energy Systems for Namibia's off- Grid Communities

Ndemuhanga V. Nghuumbwa [1], T. Wanjekeche [1,*], E. Hamatwi [1] and M. Kanime [1]

Department of Electrical and Computer Engineering, University of Namibia, Ongwediva, Namibia

* Correspondence: twanjekeche@unam.na

Abstract

Namibia's rural communities continue to experience limited and unreliable electricity access despite the country's exceptional solar, wind, and biomass renewable energy resources potential. Conventional grid extension remains financially and technically impractical for dispersed off-grid settlements, underscoring the need for cost-effective, renewable-based alternatives. This paper presents a resource-driven design and multi-objective optimization framework for Hybrid Renewable Energy Systems (HRESs) tailored to Namibia's off-grid communities. The proposed model integrates solar PV, wind turbines, biomass generators, and hydrogen-based fuel cells with hybridized energy storage consisting of batteries, supercapacitors, and hydrogen tanks. Using the Non-dominated sorting Genetic Algorithm-II (NSGA-II), the system simultaneously minimizes Total Life Cycle Cost (TLCC), Levelized Cost of Electricity (LCOE), Loss of Power Supply Probability (LPSP), Carbon dioxide (CO_2) emissions, and Wasted Renewable Energy (WRE). The framework is applied to three rural villages, Oluundje, Ombudiya, and Onguati using high-resolution, site-specific renewable resource datasets and community-level load forecasts. Results demonstrate that resource-aligned configurations substantially improve system reliability (up to 99.28%), reduce LCOE (0.0023–0.0811 USD/kWh), and optimize dispatch behavior across seasonal variations. Storage hybridization further enhances stability by balancing transient and long-duration deficits. Compared to existing diesel mini-grids, the optimized HRESs achieve markedly superior techno-economic and environmental performance. The proposed framework offers a scalable, adaptable, and policy-ready tool for accelerating sustainable rural electrification in Namibia.

Keywords: energy storage system; hybrid renewable energy system; optimization; renewable energy; rural area

1. Introduction

1.1. Background and Context

Access to reliable and affordable electricity remains one of the most pressing development challenges across the African continent. Despite significant progress in recent years, the continent's average electrification rate stands at approximately 38% [1]. This energy gap constrains socio-economic development, limits industrial productivity, and undermines efforts toward poverty alleviation and social inclusion. Rural electrification is a critical development priority, particularly in Sub-Saharan Africa where dispersed settlements, low population densities, and vast geographic distances make grid extension both technically challenging and economically prohibitive [2].

Namibia faces similar electrification challenges. Despite being richly endowed with Renewable Energy Resources (RERs), particularly solar, wind, and biomass, national electricity access stood at only 56.3% in 2020, with rural access substantially lower at 36.3% [3]. Compounding this challenge

 doi:10.20944/preprints202603.1075.v1

is the country's dependence on electricity imports, primarily coal-based power from neighbouring countries, which historically accounted for 45.8% of total supply [4]. This dependency not only exposes the country to external supply risks but also contradicts national and global commitments to the Sustainable Development Goal (SDG) 7 (Climate Action).

For remote and sparsely populated settlements, off-grid electrification using locally available Renewable Energy Sources (RESs) presents a viable, cost-effective, and environmentally sustainable alternative to traditional grid extension [2]. However, the intermittency of dominant RESs particularly solar and wind poses significant operational challenges. Without appropriate Energy Storage Systems (ESSs), RESs-based systems cannot reliably meet fluctuating load demands. Hybrid Renewable Energy Systems (HRESs), which strategically combine complementary RESs with short and long-term storage technologies have therefore emerged as the most effective solution for improving power quality, enhancing reliability, and ensuring continuous supply in off-grid environments [5]. Short-term ESSs enhance dynamic response and regulate voltage and frequency fluctuations, while long-term ESSs address extended deficits in RESs production [6], [7]. As noted by Alzahrani et al. [8], the integration of ESSs with RESs represents one of the most effective approaches for sustainable rural electrification; however, ESS technologies also introduce challenges related to cost, control complexity, operational safety, lifecycle degradation, and mobility constraints [9]. Therefore, ESS selection must account for operational characteristics, response time, economic feasibility, and serviceability requirements [8]. Considering these factors, and based on a comparative analysis of storage technologies, supercapacitors, batteries, and hydrogen storage emerged as the most suitable technologies for hybridization in off-grid Namibian communities.

Optimal sizing and configuration of HRES components are essential to achieve cost-effective designs tailored to local resource availability and community energy needs [10]. Electrification planning is inherently multi-objective, often requiring the simultaneous evaluation of economic performance, technical reliability, and environmental sustainability [11],[12]. However, many existing design tools prioritize cost minimization, neglecting equally important considerations such as reliability and environmental factors as well as their trade offs, which are especially critical in rural contexts. To address this gap, this study adopts a resource-driven design framework, emphasizing the alignment of HRES configurations with locally available RERs and community-specific demand profiles. The model supports Namibia's pursuit of SDG 7 (Affordable and Clean Energy) and 13 (Climate Action) to facilitate long-term socio-economic development in rural communities.

1.2. Academic Perspective and Need for Research

While PV-battery configurations are technically feasible, they often require very large Battery Energy Storage System (BESS) capacities to reach 100% renewable penetration, making them prohibitively expensive [13]. The addition of complementary resources such as wind can reduce battery cycling and lower the LCOE, yet batteries alone remain constrained by limited cycle life and high replacement costs [14], [15]. Consequently, studies exploring multi-storage combinations such as PV/BESS/supercapacitors (SCs) [16] and PV/fuel-cell (FC)/SC systems [17] consistently demonstrate that supercapacitors are effective for smoothing high-frequency fluctuations, while fuel cells provide long-duration support during extended low-generation periods. These findings collectively confirm that no single storage technology can meet the dynamic and multi-timescale requirements of high-RES microgrids; rather, an optimal blend of short-term and long-term storage is essential for cost-effective and reliable operation.

A review of previous case studies reveals wide variation in load demand assessment methodologies. Some studies adopt holistic or simulated load profiles that reflect weekday–weekend differences and seasonal variations such as summer and winter peaks [18], [19]. More sophisticated models incorporate socio-economic and behavioural uncertainty using stochastic techniques, including Markov Chain Processes [20] and bottom-up RAMP-based modelling [21].

 doi:10.20944/preprints202603.1075.v1

Empirical studies targeting institutions (e.g., schools, clinics) capture seasonal variability by load type [22], whereas community-level surveys such as those conducted in Oluundje, Namibia [23] provide realistic data but often ignore inter-seasonal variations. Conversely, simplified forecasting models that assume constant daily loads across seasons, as in Amarika, Namibia [24].

Given the complexity of accurately modelling both supply and demand, optimal HRES sizing requires tools and techniques that can evaluate multiple conflicting objectives simultaneously. Typical objectives span economic (e.g., LCOE), technical (e.g., reliability), environmental (e.g., emissions), and social considerations such as affordability and local resource utilization [25].

Despite their widespread use, existing software tools for HRES planning present notable limitations. HOMER, the most used platform for sizing and economic evaluation, supports simulation and sensitivity analysis but lacks capabilities for true multi-objective optimization and cannot model critical factors such as battery depth of discharge or environmental indicators [26], [27]. Other tools, HYBRID2, HYBRIDS, TRNSYS, RETScreen, and PVsyst offer specialized features but suffer from some constraints. HYBRID2 requires extensive datasets and lacks flexibility, TRNSYS and HYBRIDS simulate transient behaviour but cannot determine optimal sizing, RETScreen supports financial and emissions analysis but does not model temperature effects on PVs, and PVsyst excels in PV modelling but lacks hybrid system optimization capabilities [140]. These limitations collectively indicate that generic tools are insufficient for designing systems for rural Namibian communities that align with SDG 7 and 13.

As a result, literature increasingly favours advanced optimization methods, particularly heuristic and metaheuristic algorithms that can efficiently explore non-linear, multi-dimensional search spaces. Dad and Saleem [28] identified a wide range of techniques used in HRES optimization, from analytical and iterative methods to probabilistic, graphical, and Artificial Intelligence (AI) based approaches. Analytical methods benefit from simplicity but struggle with non-linear formulations [29], while iterative methods are intuitive yet often slow to converge [30]. Graphical techniques are easy to interpret but limited to two variables [31], Consequently, Genetic Algorithms (GA), Particle Swarm Optimization (PSO), Simulated Annealing (SA), and Artificial Neural Networks (ANN) have become the preferred choice for addressing the inherent non-linearity and uncertainty of HRES design.

Maheri [32] asserts that the three dominant uncertainties, renewable resource variability, parameter uncertainty in cost and power models, and unpredictable human behaviour, necessitate the use of algorithms capable of global search and robust handling of stochastic inputs. For single-objective problems, algorithms such as PSO, GA, SA, Ant Colony Optimization, Harmony Search, and Bee Swarm Optimization have been applied. For multi-objective optimization, NSGA-II, NSGA-III, and Multi-Objective PSO (MOPSO) are the most widely adopted.

Comparative studies show distinct strengths. MOPSO generally offers faster convergence and better uncertainty handling, while NSGA-II produces more accurate and diverse Pareto fronts. Shaha et al. [33] found that MOPSO yields lower Loss of Power Supply Probability (LPSP), whereas NSGA-II results in lower LCOE. Similarly, for solar–wind–battery systems, MOPSO converges faster, but NSGA-II provides superior Pareto diversity [34]. In systems incorporating hydrogen technologies, both NSGA-II and MOPSO perform comparably in achieving high Primary Energy Saving Ratios (PESR) [35].

1.3. Gap in the Research and Novelty of the Presented Work

Although various tools and models have been applied to HRES design, most existing approaches still fall short of capturing the full multi-dimensional nature of rural electrification planning. They rarely integrate cost, reliability, environmental impact, and multi-storage dynamic within a unified optimization framework.

These limitations underscore the need for more comprehensive methods capable of jointly exploring the trade-offs among economic, technical, and environmental objectives under varying rural resource and demand conditions. To address this gap, the present study develops a multi-

 doi:10.20944/preprints202603.1075.v1

objective optimization model based on the weighted NSGA-II algorithm to simultaneously minimize TLCC, LCOE, LPSP, WRE and CO_2 emissions. The proposed framework integrates multi RESs (SPV, wind, biomass, and fuel cells) together with complementary storage technologies including batteries, supercapacitors, and hydrogen storage, enabling robust performance across both transient and steady-state operating conditions

The novelty of this work lies in the development of a customized adaptive NSGA-II approach combined with a weighted Pareto based mechanism, allowing systematic evaluation of trades offs across the five objectives. The model is applied to three rural Namibian communities (Oluundje, Ombudiya, and Onguati), with differing resource availability and load characteristics, demonstrating its scalability, adaptability, and suitability for real-world electrification planning.

2. Renewable Energy Resources Analysis

2.1. Wind Speed Analysis

Using the seasonal histograms given in Figure 1 with wind speed distribution of 0.5 m/s wind bins for the three rural areas, it is confirmed that winter is the most favorable season with the lowest null wind (<2.5 m/s) percentages, and summer is typically the least favorable (highest null wind) as it is further be summarized in Table 1. These seasonal patterns underscore the need for hybridization and storage to manage intra-day and seasonal supply variations.

Table 1. Average Percentage of Wind Speed (< 2.5 M/S) in Each Village for Every Season.

Village	Wind speeds < 2.5 m/s).in %			
	Summer	Spring	Winter	Autumn
Oluundje	17.1	15.82	12.1	9.02
Ombudiya	15.62	14.43	9.48	9.08
Onguati	29.76	17.22	12.68	28.63

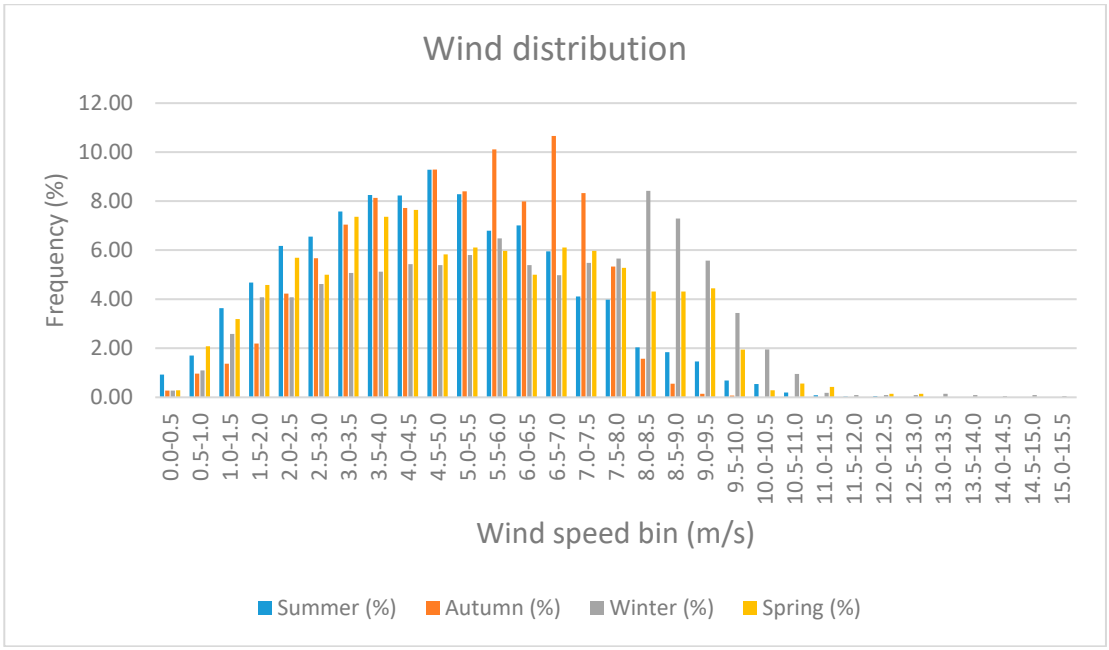

(**a**)

 doi:10.20944/preprints202603.1075.v1

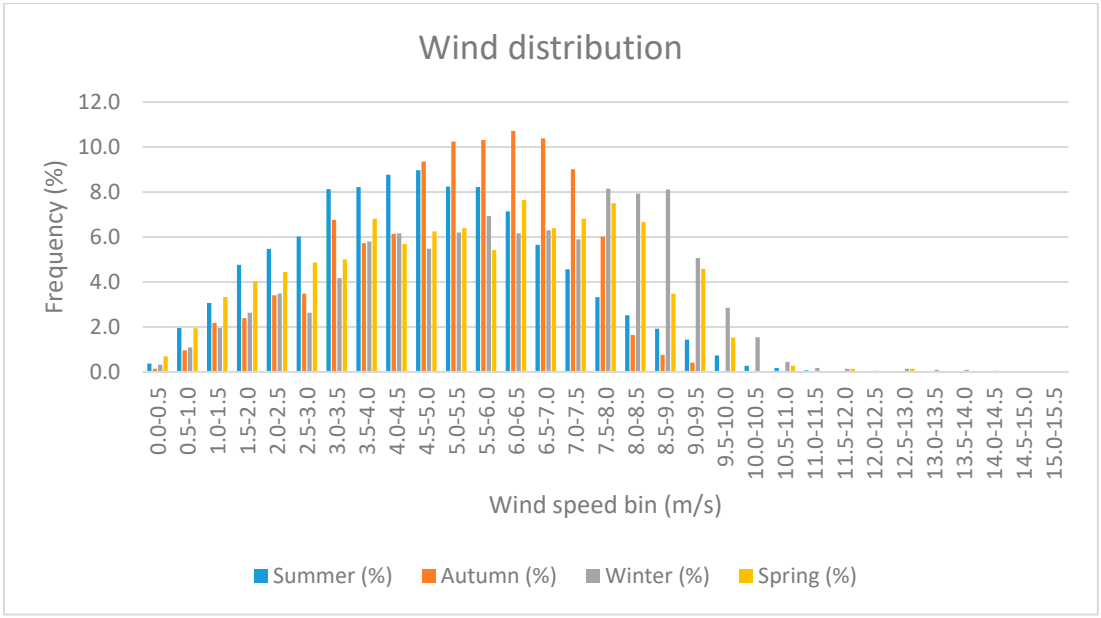

(**b**)

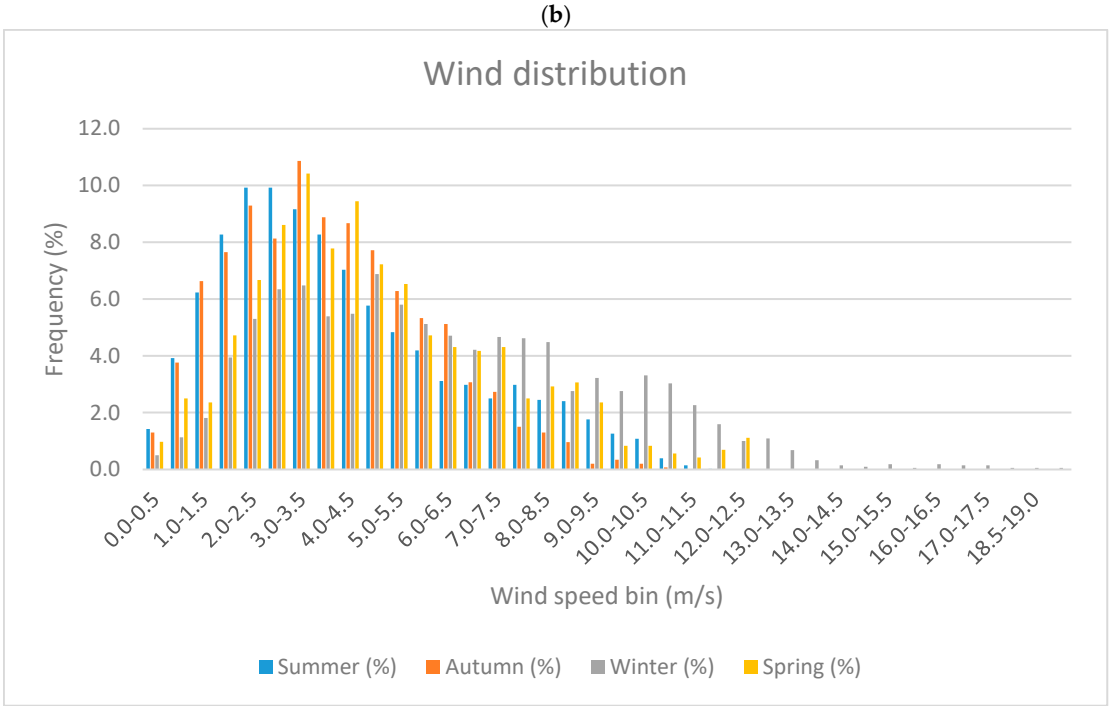

(**c**)

Figure 1. Seasonal wind speed distribution frequency for (**a**) Oluundje, (**b**) Ombudiya and (**c**) Onguati villages.

2.2. Solar Irradiance Analysis

Solar PV (SPV) converts irradiance to electricity and is strongly influenced by Global Horizontal Irradiance (GHI) and cell temperature. A minimum solar insolation needed to generate electricity is 100–200 W/m² [36]. The solar resources of the three rural areas were assessed based on the re-analysis data obtained from the National Aeronautics and Space Administration (NASA) as provided in Figure 2.

 doi:10.20944/preprints202603.1075.v1

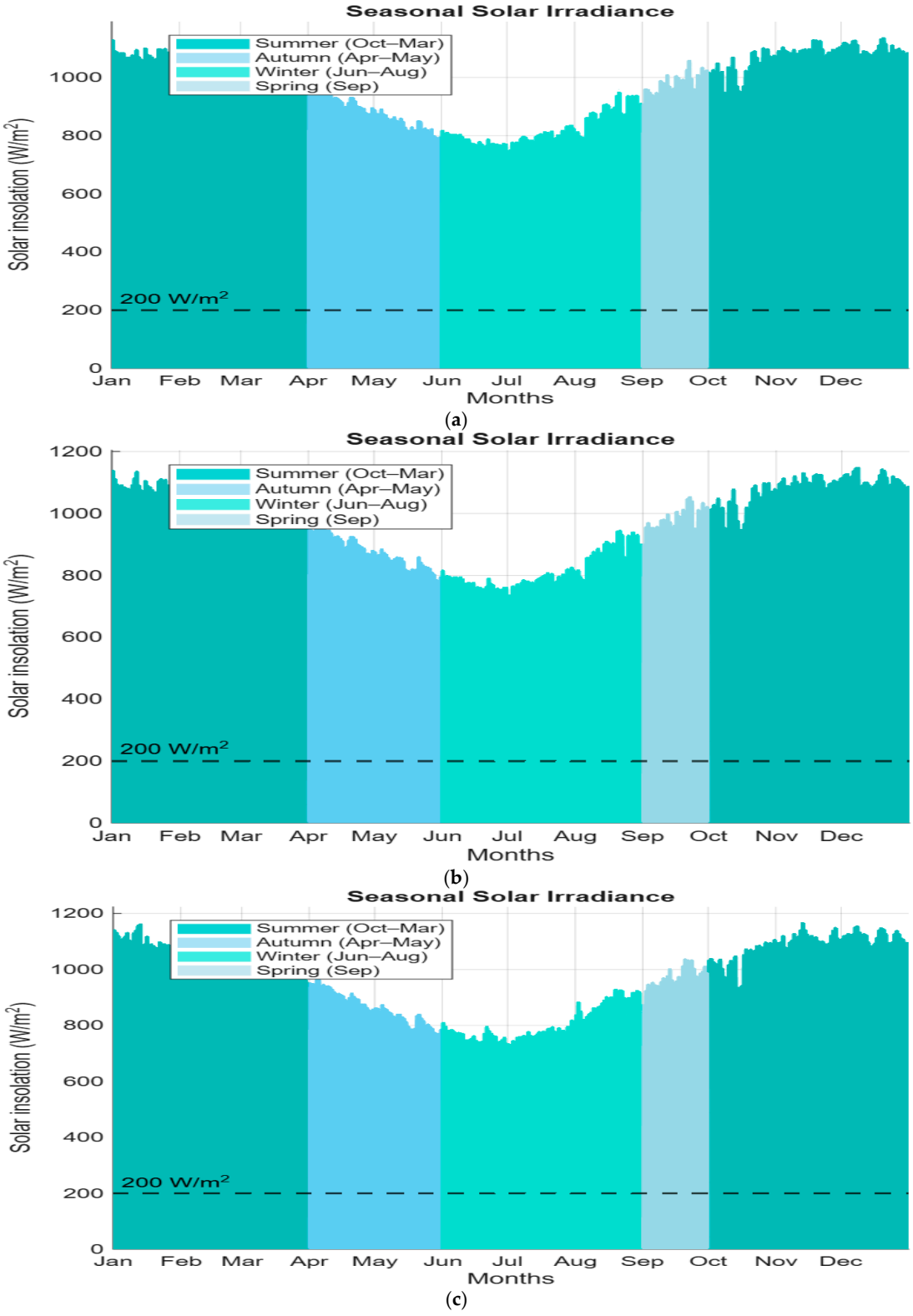

Figure 2. Winter, Summer, Autumn and Spring Solar Irradiance for (**a**) Ombudiya, (**b**) Oluundje and (**c**) Onguati.

The solar irradiance assessment for the three villages, Ombudiya, Oluundje, and Onguati, reveals strong and consistent solar energy potential throughout the year, as illustrated in Figures 2 (a), (b) and (c), respectively. Specifically, summer exhibits the highest irradiance levels, with peak GHI values exceeding 1,076.35 W/m² in Ombudiya, 1,093.7 W/m² in Oluundje, and 1,104.53 W/m² in Onguati. Spring also demonstrates strong irradiance, averaging between 980 W/m² and 1,000 W/m², followed by autumn, which presents slightly lower peaks (around 820–950 W/m²). Observably,

 doi:10.20944/preprints202603.1075.v1

winter exhibits the lowest solar intensity, with irradiance values of approximately 780–790 W/m², though still well above the minimum PV-operational threshold of 200 W/m².

The annual and seasonal GHI profiles indicate high solar stability with minor seasonal variations, affirming the feasibility of year-round photovoltaic generation. However, absence of irradiance during the morning and night time highlight the necessity of energy storage systems or hybrid operation (e.g., with wind or biomass) to maintain supply continuity during non-solar irradiance hours.

2.3. Biomass Resources

Table 2 illustrates the biomass power generation potential of the three sites. It can be observed that Oluundje and Ombudiya villages have higher biomass resources compared to the Onguati village. This plays a significant role in hybrid configurations as will be illustrated in the subsequent sections.

Table 2. Biomass resources of the three rural Areas.

Village	Area(ha)	Resource (dry tonnes/year)	Resource (kWh/year) (only 30% of resource)
Oluundje	2342	1011.74	1518346.2
Ombudiya	3038.8	1312.76	1969140
Onguati	4663.6	91.58	137370

This section has provided an overview of the available RERs, highlighting their availability and variability for rural electrification in Namibia. The discussion emphasized the variability and complementarity of solar, wind, and biomass resources.

2.4. Modelling of Hybrid Renewable Energy System

(a) System Overview

Mathematical formulations and simulation procedures for solar PV, wind turbines, and biomass gasifiers, along with the corresponding energy storage systems (battery, supercapacitor, and fuel cell). The models incorporate key environmental, operational, and design parameters to ensure realistic performance evaluation. Furthermore, the subsection outlines the methodology used to estimate and forecast energy demand for the rural communities

(b) Solar Power Model

SPV output power is determined using Eq. (1) [37]:

$$P_{pv} = \eta_{pv} A_{pv} G_T [1 - 0.005\ (T_c - 25)] \quad (1)$$

Where η_{pv} is the photoelectric efficiency in (%), A_{pv} is the area of the PV array in (m²), G_T (1000 W/m²) is the incident solar radiation and Tc (◦ C) is the cell operation temperature [37]. The GHI is used for SPV G_T. Using GHI and ambient temperature, module temperature is as given in Eq. (2)[37], [38]:

$$T_c = T_a + \frac{T_{NOCT} - 20}{800} G_T \quad (2)$$

T_c and T_a denote cell temperature and ambient temperature respectively, and T_{NOCT} is nominal operating cell temperature [37]. The T_{NOCT} value is in the range of 45± 3 C, based on the climate condition of the state [38].

(c) Wind Power Model

Wind output power is determined using Eq. (3)[39]:

 doi:10.20944/preprints202603.1075.v1

$$P = \begin{cases} P_r, & if\ V_r < v(t) < V_{co} \\ P_r \dfrac{v^3(t) - V^3{}_{ci}}{V^3{}_r - V^3{}_{ci}}, & if\ V_{ci} < v(t) < V_r \\ 0, & v(t) \le V_{ci}\ or \\ & v(t) \ge V_{co} \end{cases} \quad (3)$$

Pr is the rated power, and $v(t)$, V_{ci}, V_{co}, V_r are the actual, cut-in, cut-out and rated wind speeds (m/s), respectively. The rated power is defined as a function of the area swept by the wind turbine blades (A_w), air density (ρ_a) (1.225 kg/m^3), power coefficient (C_p), wind turbine generator efficiency (η_g) and the rated velocity (V_r) as indicated in Eq. (4)[39]:

$$P_r = \frac{1}{2}\rho_a A_w \eta_g\, C_p V^3{}_r \quad (4)$$

The theoretical maximum value of the power coefficient C_p is 0.593, also known as the Betz's coefficient [40].

(d) Biomass Power Modelling

Biomass gasification generator power is determined using Eq. (5)[41], [42].

$$P_{BMG} = \frac{Total\ fuel\ wood\ \left(\frac{ton}{yr}\right) \times Calorific\ value_{BM} \times \eta_{BMG} \times 1000}{365 \times 860 \times (operating\ hours\ per\ day)} \quad (5)$$

η_{BMG} is the efficiency of the biomass generator.

(e) Battery Storage System Model

The equations used for the mathematical modelling of the battery outlined in [43] is as given in equation 6 illustrating Battery State of Charge (SOC).

$$z(t) = z(t_O) - \frac{1}{Q}\int i(T)d(T) \quad (6)$$

$z(t)$ represents the SOC at time t, expressed in seconds, $z(t_O)$ represents the initial SOC value, $\frac{1}{Q}$ represents the battery capacity, and $i(T)$ is the current through the battery expressed in (A). $i(T)$ is positive for the discharging cycle and negative for the charging cycle, as illustrated in Eq. (7)–(8).

Discharging equation ($i* > 0$)

$$V_{bat} = f_1(it, i*, i) = E_O - K\frac{Q}{Q - it}i* - K\frac{Q}{Q - it} + Aexp(-B.it) \quad (7)$$

Charging equation ($i* < 0$)

$$V_{bat} = f_2(it, i*, i)) = E_O - K\frac{Q}{it + 0.1Q}i* - K\frac{Q}{Q - it} + Aexp(-B.it \quad (8)$$

where V_{bat} is the battery voltage in volts, i is the battery current in amperes, t is the time in seconds, V_O is the constant battery voltage in volts, Q is the maximum battery capacity in ampere-hour, A is the exponential voltage in volts, B is the exponential zone time constant inverse (Ah)$^{-1}$, it is actual battery capacity (Ah), $i*$ is low frequency current dynamics and K is the polarisation constant in (Ah)$^{-1}$.

(f) Capacitance Model

The capacitance of the supercapacitor is determined using Eq. (9)[44]:

$$C = \frac{2W}{(0.9\ U_R)^3 - (0.7\ U_R)^3} \quad (9)$$

 doi:10.20944/preprints202603.1075.v1

where C is the Capacitance, W is the discharge energy between start and end voltages and U_R is the rated voltage of the supercapacitor.

(g) Fuel Cell Model

Fuel cells operate on the opposite principle of water electrolysis. The cells work on the premise of recovering the combustion energy of hydrogen and converting it into electrical energy at each electrode through Eq. (10) and (11) (chemical reactions) [45].

Anode reaction:

$$H_2 = 2H^+ + 2e^- \tag{10}$$

Cathode reaction:

$$2H^+ + 2e^- + \frac{1}{2}O_2 \rightarrow H_2O + heat \tag{11}$$

The total voltage produced by the fuel cell (FC) is determined using Eq. (12) [96]:

$$V_{FC} = E_{Nernst} - V_{act} - V_{ohmic} - V_{con} \tag{12}$$

Whereas for cells connected in series and forming a stack, the voltage is determined by Eq. (13):

$$V_s = n \times V_{FC} \tag{13}$$

E_{Nernst} is thermodynamic potential of each unit cell and represents its reversible voltage, V_{act} is voltage drop associated with the activation of the anode and of the cathode, V_{ohmic} is ohmic voltage drop associated with the conduction of protons and electrons, V_{con} is voltage drop resulting from the decrease in the concentration of oxygen and hydrogen.

(h) Hydrogen Storage Tank Model

According to the gas-state equation, internal pressure of a hydrogen tank is determined using Eq. (14)–(16):

$$P_{tank} = \frac{\eta_{H_2} R T_{tank}}{V_{tank}} \tag{14}$$

$$\eta_{H_2}(t_o + \Delta t) = n_o(t_o) + \int_{t_o}^{t_o+\Delta t} q_{H_2} dt \tag{15}$$

$$q_{H_2 = W_{elec} - W_{fc}} \tag{16}$$

P_{tank} is the tank pressure; nH_2 is the amount of hydrogen in the tank; V_{tank} is the volume of tank; R is the molar gas constant; T_{tank} is the gas temperature; n_0 (t_0) is the initial value of the substance inside the gas tank at time t_0; qH_2 is the net hydrogen feed flow rate; and W_{fc} is the hydrogen flow rate at a gas tank outlet.

(i) Load Model

The mathematical models adapted in this study to forecast the aggregated load demand is provided in eq (17) and (18).

$$D_h = \sum_{j}^{Userclass} N_j \sum_{i}^{Appliance} n_{ij} P_{ij} \tag{17}$$

$$D_d = \sum_{h=0}^{23} D_h \tag{18}$$

where h is the hour of the day [h = 0,1,2,3,…23], i refers to the type of electrical appliances and j refers to the type of consumer, N_j is the number of users and n_{ij} is the type of appliance of each

 doi:10.20944/preprints202603.1075.v1

consumer class (TVs, lights, phones, etc.,), P_{ij} represents the nominal power of the different types of appliances of each consumer, D_d is the total daily load demand of the entire system, D_h is the hourly load demand of the entire system.

2.5. Problem Formulation

Objective functions are crucial components in the optimization of HRESs, as they guide the search for optimal solutions by quantifying system performance. According to Sharma and Kumar [46], objective functions are computable mathematical expressions that evaluate the quality of candidate solutions based on decision variables. In this study objective function are derived using Eq. (19)–(20):

$$F(x) = (f_1(x), f_2(x), f_3(x), f_4(x), f_5(x)) \tag{19}$$

where k is the number of objective functions, and each function $f_i(x)$ represents a specific performance criterion. In addition, the different objective functions for this study are divided into financial, technical and environmental functions and are described for modelling as follows:

Financial objectives

$$f_1(x): Minimise\ Total\ Life\ Cycle\ Cost\ (TLCC)$$
$$f_2(x): Minimise\ Levelized\ Cost\ of\ Electricity\ (LCOE)$$

Technical objectives

$$f_3(x): minimise\ Loss\ of\ Power\ Supply\ Probability\ (LPSP)$$
$$f_4(x): Minimise\ Wasted\ Renewable\ Energy\ (WRE)$$

Environmental objectives:

$$f_5(x): Minimise\ total\ CO_2\ emission\ (\frac{CO_2\ emission}{kg})$$

The overall objective function is further modelled as follows:

Objective function: Min ($TLCC, LCOE, LPSP, WRE, CO_{2,emission}$).

$$\begin{aligned}&\text{Min}(\sum_{s=1}^{S}\left(C_i + \sum_{t=1}^{T}\left(\frac{O_t + M_t + F_t}{(1+r)^t}\right) + C_d\right), \sum_{s=1}^{S}\left(\frac{I_{cost} + \sum_{t=1}^{T}\frac{O_t \& M_t (1+g)^{t-1} + F_t}{(1+r)^t}}{\sum_{t=1}^{L_s}\frac{E_t}{(1+r)^t}}\right),\\ &\frac{\sum_j^N (P_L(t) - P_{tot_{sys}}(t))}{\sum_j^N (P_L(t)}, \sum_{t=1}^{T} P_{wasted}(t)\ ,\\ &\sum_{t=1}^{T} CO_{2,emission})\end{aligned} \tag{20}$$

where t is the time in years, C_i is the initial investment capital, O_t is the operational cost with respect to time t, M_t is the maintenance cost with respect to time t, F_t is the fuel cost with respect to time t, S is energy sources, r is the discount rate, g is the annual growth rate of $O\&M$ expenditure, E_t is the electricity generated in year t, $P_{wasted}(t)$ is WRE in year t, and $P_{syst}\ tot$ is the total power of the system.

Eq. (21)–(35) define the operational and design constraints necessary for optimizing the HRES. Optimization ensures minimized LPSP, reduces energy waste, and maintains the state of charge of storage systems (battery and supercapacitor) within safe bounds. The constraints also regulate the sizing of system components, enforce realistic limits on the use of renewable resources, and guarantee the presence of essential system elements like fuel cells and hydrogen storage. Finally, the reliability constraint (shown in Eq. (35)) ensures that the system achieves power supply with LPSP above minimum thresholds, thereby prioritizing reliability in rural electrification scenarios.

(a) Equalities Constraints

(i) Power Balance Equality Constraints

The power balance equality is determined by Eq. (21).

$$P_L(t) - \left(P_{C_{SPV}}(t) + P_{C_{WG}}(t) + P_{C_{BMG}}(t) + P_{C_{BAT}}(t) + P_{C_{SC}}(t) + P_{C_{FC}}(t)\right) = P_{imb}(t) \quad \forall t$$

Where if: $P_{imb}(t) > 0$: $Demand\ exceeds\ supply\ (deficit)$,
$P_{imb}(t) < 0$: $Supply\ exceeds\ demand\ (surplus)$,
$P_{imb}(t) = 0$: $Perfect\ balance$ (21)

 doi:10.20944/preprints202603.1075.v1

$P_L(t), P_{C_{SPV}}(t), P_{C_{WG}}(t), P_{C_{BMG}}(t), P_{C_{BAT}}(t), P_{C_{SC}}(t)$, and $P_{C_{FC}}(t)$ represent the load, SPV, wind generator, biomass generator, battery, supercapacitor and fuel cell power at time t, respectively, with respect to the optimized capacities, and $P_{imb}(t)$ *is power imbalance at time* t .

(ii) Wasted Power Equality Constraints

The total wasted renewable energy is determined by Eq. (22) and (23).

$$P_{C_{SPV}}(t) + P_{C_{WG}}(t) - (P_L(t) + P_{C_{BAT}}(t) + P_{C_{SC}}(t)) = P_{wasted}(t)\ \forall t \tag{22}$$

$$P_{wasted\_total}(t) = \sum_{t=1}^{T} P_{wasted}(t) \tag{23}$$

where $P_{wasted}(t)$ is the wasted power at time t and $P_{wasted\_total}(t)$ is the total wasted power.

(b) Inequalities Constraint

(i) Storage System Operational Inequality Constraints

Equation (24)–(27) is used to provide the operating limits of the battery, supercapacitor, hydrogen storage tank and biomass storage, respectively.

$$SOC_{BAT,MIN}(t) \le SOC_{BAT} \le SOC_{BAT,MAX}\ \forall t \tag{24}$$

$$SOC_{SC,MIN}(t) \le SOC_{SC} \le SOC_{SC,MAX} \quad \forall t \tag{25}$$

$$C_{H_2,storage}(t) \ge 0 \quad \forall t \tag{26}$$

$$Biomass_{storage}(t) \ge 0 \quad \forall t \tag{27}$$

where SOC_{BAT} and SOC_{SC} represent the state of charge of the battery and supercapacitor, respectively. Whereas $C_{H_2,storage}(t)$ and $Biomass_{storage}(t)$ represent the hydrogen and biomass storage capacities, respectively.

(ii) Renewable Energy Sizing Inequalities Constraint

Equation (28)–(30) presents the sizing constraints of solar, wind turbine and biomass generator, respectively.

$$C_{SPV} \ge 0 \quad \forall t \tag{28}$$

$$C_{WG} \ge 0 \quad \forall t \tag{29}$$

$$C_{BMG} \ge 0 \quad P_{BMG} \le P_{BMG,MAX} \quad \forall t \tag{30}$$

where C_{SPV}, C_{WG}, and C_{BMG} are the capacity of SPV, wind and biomass generation.

(iii) Storage Sizing Inequalities Constraint

Eq. *(31)–(34)* presents the sizing constraints of the battery, supercapacitor, hydrogen fuel cell and hydrogen storage tank, respectively.

$$C_{BAT} \ge 0 \quad \forall t \tag{31}$$

$$C_{SC} \ge 0 \quad \forall t \tag{32}$$

$$C_{FC} \ge 0 \quad \forall t \tag{33}$$

$$C_{H_2,storage} \ge 0 \quad \forall t \tag{34}$$

where C_{BAT}, C_{SC}, C_{FC}, and $C_{H_2,storage}$ represent the capacities of the battery, supercapacitor, fuel cell and hydrogen storage tank respectively.

(iv) Reliability Equality Constraint

Eq. (35) presents the LPSP operating constraint

 doi:10.20944/preprints202603.1075.v1

$$LPSP \geq 0 \qquad \forall t \qquad (35)$$

2.5. Proposed Energy Management Strategy

HRESs consisting of multiple energy sources are increasingly investigated to provide reliable and uninterrupted power supply in remote or islanded microgrids. However, to ensure the efficient and safe operation of such systems, a robust Energy Management Strategy (EMS) is essential. The EMS governs the coordination of energy sources, controls power generation and distribution, and regulates the charging and discharging behavior of ESSs, ensuring system reliability and performance under varying operational conditions. As emphasized in [47] and [48], the development of an EMS must consider load behavior, the nature of energy sources, and their availability to ensure technical feasibility, economic efficiency, and long-term system reliability. Additionally, EMSs play a critical role in maintaining power balance under fluctuating generation conditions, particularly in isolated microgrids [49].

While numerous studies have focused on the techno-economic sizing of HRES components, many neglect operational dispatch strategies [48]. However, subtle adjustments to control logic can substantially improve system dynamics. According to Sanaa et.al [49], careful alignment of energy production, consumption, and storage methodology enhances system responsiveness, stability, and efficiency, especially during transients or periods of resource unavailability.

Given the centralized configuration of the proposed system and the goal of integrating sizing and dispatch control within a unified framework, this study adopts a deterministic rule-based EMS guided by a Multi-Objective Optimization approach (NSGA-II). This hybrid strategy enables optimal component sizing while ensuring real-time operational flexibility, energy balancing, and protection of critical components [48].

(a) Objectives of the Proposed Energy Management Strategy

Taking into consideration the intermittency of the RERs and the unpredictable load variations, the proposed EMS aims to achieve the following:

(i) Ensure reliable and continuous supply of power to the loads depending on power availability.
(ii) Ensure efficient operation of the different RESs and HESS.
(iii) Reduce hybrid system operational cost.
(iv) Avoid overcharging and over discharging of the battery and ultracapacitors.

Factors taken into consideration for the proposed EMS

The effectiveness of the proposed EMS is evaluated in terms of reduction of LPSP, and reducing operation cost, ESSs and the greenhouse gas emission of systems, therefore the following factors are taken into consideration:

- **Wind and Solar:** Since the prediction of the power output from these RESs is challenging and cannot be dispatched at will, it is recommended for utilization when available or stored for later use.
- **Load following strategies:** Fuel Cell energy production and Biomass energy production.
- The model combines real time PV and wind power information, considers the limitation of the SOC of the HESS, adjusts the charge or discharge power of ESSs in real time, and optimises the working state of different energy storage components.

(b) Modes Of Operation of The Hybrid Energy Sources System

Mode 1: Wind and solar energy are produced to maximum capacity as per their availability

(i) The batteries and supercapacitors are charged during this mode with relation to the RESs generation and load demand provided that $SOC \leq SOC_{max}$.
(ii) The dump load is activated during this mode if $SOC = SOC_{max}$ for both the batteries and supercapacitors, and there is still excess energy in the network.

 doi:10.20944/preprints202603.1075.v1

Mode 2: Supercapacitors have high power densities and tolerate a large number of rapid charge–discharge cycles as compared to batteries [50]. Therefore, in this study, the supercapacitor is available for transient responses to absolve or provide peak currents, and it is used to respond to rapid load and RESs generation variations when the generated power by the RESs is lower or higher than the load demand.

Mode 3: Battery bank is used to supply long term power and cater for low frequency load and RESs variations and for transient responses.

Mode 4: The fuel cell is used to supply long term power when the batteries are discharged beyond or equivalent to SOC_{min} or when the batteries cannot fully supply the load.

(i) The batteries and supercapacitors are not charged during this mode.

(ii) The dump load is not activated during this mode.

Mode 5: Biomass generator is used to supply long term power when the batteries and fuel cell resources are deployed beyond their minimum thresholds, or when these resources cannot fully supply the entire load.

(i) The batteries and supercapacitors are not charged during this mode

(ii) The dump load is not activated during this mode.

Mode 6: When the total generation from all the RESs and ESSs cannot fully supply the load, and the power is sufficient to supply the critical load, then only the critical load will be supplied, otherwise the power from wind and solar will be used to charge the battery and supercapacitor and no load will be supplied during that period.

(c) Proposed Energy Management Flow Chart

To further demonstrate the energy flow management of the microgrid, the proposed energy management flowchart is provided in Figure 3.

2.6. Proposed Optimization Algorithm

The NSGA-II algorithm, introduced by Deb et al. in 2002, overcomes limitations of the original NSGA by introducing elitism, fast non-dominated sorting, and crowding distance comparison [33,51]. NSGA-II is widely recognized for its computational efficiency and is extensively used as a benchmark for evaluating new optimization methods. Unlike other algorithms such as MOPSO, NSGA-II handles complex multi-dimensional problems with higher stability but may require more time to converge.

Given the limitations of existing tools and the need for high-accuracy, customized optimization for rural electrification in Namibia, this study proposes the development of a multi-objective, NSGA-II-based optimization model. The model is tailored to local energy resource data, socio-economic characteristics, and policy frameworks. Its goal is to ensure reliable, cost-effective, and environmentally sustainable electrification aligned with national development goals and SDG 7 and 13. The adapted NSGA-II algorithm is presented as follows:

Algorithm 1: The Proposed NSGA-II for HRES

Inputs:

1: N=10 (population size).

2: G=10 (number of generations).

3: Decision vector

X = [P_{PV}, P_{Wind}, P_{Bio}, E_{Bat}, E_{SC}, P_{FC}, H_2^{max}, Inv_{size}, …]

4: System parameters: efficiencies (η_{PV}, η_{Wind}, η_{Bio}, η_{FC});

SOC limits ($SOC_{SC}^{min}=0.2$, $SOC_{SC}^{max}=0.9$; $SOC_{Bat}^{min}=0.2$, $SOC_{Bat}^{max}=0.8$);

Hydrogen bounds [H_2^{min}, H_2^{max}]; yearly biomass cap.

5: Termination: stop after G generations.

6: Random seed fixed; log best LCOE every 5 generations.

Objectives (all minimized):

7: $f1 = LCOE(X)$

 doi:10.20944/preprints202603.1075.v1

8: $f2 = TLCC(X)$
9: $f3 = 1 - \text{Reliability}(X)$: Reliability inverted so that minimization favors higher reliability
10: $f4 = CO_2$ Emissions(X)
11: $f5 = -$Wasted Power(X): Wasted renewable energy inverted so that minimization favors lower curtailment

12: Initialization Phase
13: Generate N feasible solutions
$P=\{X_1,\ldots,X_N\}$
Using generate_random_solution().
14: Apply repair_individual() (round P_{Bio} to 100 kW, P_{FC} to 6 kW, enforce bounds).

15: **Fitness Evaluate**
16: For each $Xi \in P$:
17: Run hourly EMS dispatch simulation.
18: Compute
$F(X_i) = [f_1, f_2, f_3, f_4, f_5]$

19: Non-Dominated Ranking
20: Apply fast non-dominated sorting → fronts F_1, F_2,…
21: Compute crowding distance in each front.

22: Main Evolutionary Loop
23: For generation g = 1 to G do
24: Selection and Reproduction
25: Initialize Q = ∅.
26: While |Q|<N do
27: Select parents via tournament (size = 3).
28: Uniform crossover with $p_c = 0.9$ else clone.
29: Mutation per gene with rate 0.80:
→ $X' = X \times (0.4+0.7\cdot\text{rand})$.
30: Repair offspring; add to Q.
31: End while
32: Environmental Selection
33: Combine R = P ∪ Q.
34: Non-dominated sort R → F_1, F_2 ,….
35: Fill P_{next} with successive fronts until $|P_{next}|=N$.
36: If last front overfills: select by highest crowding distance.
37: Progress Logging
38: If $g \ mod 5 = 0$, record min ($f1$) in P_{next}.
39: Set $P \leftarrow P_{next}$.
40: End for

41: Termination
42: Return final Pareto set F_1 from generation G.

43: Weighted Decision-Making
44: Normalize objective values for all $Xi \in F_1$.
45: Assign weighting factors reflecting rural-electrification priorities:
– LCOE = 0.35; Reliability (LPSP) = 0.35; Emissions = 0.10; Wasted Power = 0.20
46: Compute weighted score:
$\text{Score}(Xi)=0.35\, f_{norm}^{LCOE}+0.35 f_{norm}^{LPSP}+0.10\, f_{norm}^{CO2}+0.20 f_{norm}^{WRE}$
47: Select final preferred configuration
$X^* = \arg \max_{Xi \in F1} \text{Score}(Xi)$

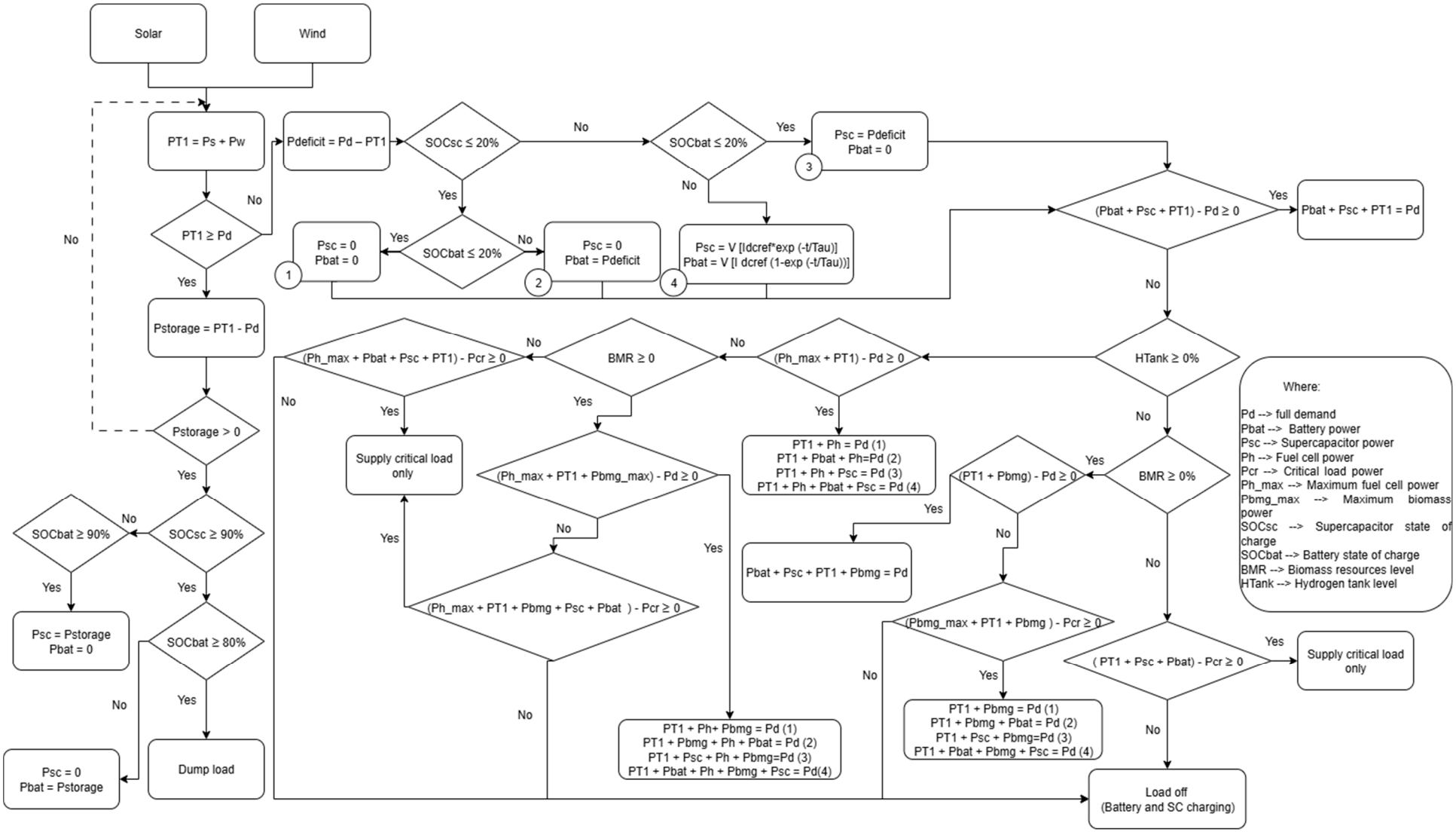

Figure 3. Flow chart of the proposed energy management flow chart.

 doi:10.20944/preprints202603.1075.v1

2.6. Simulation Results

This section presents and analyzes the results obtained from the optimization of hybrid renewable energy systems for the selected rural communities; Oluundje, Ombudiya, and Onguati. The results are discussed in terms of system performance, seasonal power variations, and the behavior of storage components. It also evaluates the Pareto-optimal solutions, comparing trade-offs among technical and economic objectives. The analysis further explores energy compositions, capacity factors, and dispatch characteristics under different operating scenarios. This comprehensive assessment provides valuable insights into the viability of renewable-based microgrids in Namibia.

(a) Optimal Solution

This section presents the optimal sizing configurations for the HRESs of the three selected villages; Oluundje, Ombudiya, and Onguati, based on the NSGA-II multi-objective optimization algorithm. The optimization process balances conflicting objectives, such as minimizing LCOE, reducing emissions, maximizing reliability, and minimizing wasted renewable energy. Each village's energy configuration was modeled and simulated in MATLAB/Simulink. The Pareto optimal solutions for each area are provided in the subsequent subsections, which are further weighted and the Pareto solution with the highest score is chosen as the best solution. The best solution is indicated with a yellow star in the graph of Optimal output of Reliability vs. LCOE vs. Wasted power, based on weighted Pareto (Figure 4–6(b)), and with a red rectangle in the Pareto optimal solution tables (Figure 4–6 (a)) as well as in the weighted Pareto optimal solutions tables (Figure 4–6 (c)).

Figure 4 illustrates the Pareto optimal solutions for Oluundje village, showcasing multiple trade-off solutions between cost, emissions, reliability, and wasted energy. From Figure 4(b), the best solution highlighted with a red rectangle achieves the highest weighted score of 0.9100, combining 99.28% reliability, TLCC of 849173.00 USD, and a low LCOE of 0.0042 USD/kWh. This optimal configuration includes significant contributions from solar (26.10 kW) and wind (177.09 kW). Notably, the biomass allocation is substantial (100.00 kW), confirming its dominance in this village's generation mix, and this is in agreement to the findings of [51], that biomass is one of the least-cost energy sources for mini-grids, especially in villages with more than 200 households and electricity demands exceeding three hours per day. The fuel cell (60.00 kW) serves a complementary role, with battery and supercapacitor capacities of 180.93 kWh and 2.56 kWh, respectively, indicating a need for both long-term and fast-response storage.

In Figure 5, the best Pareto optimal solution for Onguati village reveals a markedly different optimal mix due to its higher wind potential as compared to other renewable energy sources in conjunction to the areas of low load demand, with a reliability of 94.20%, LCOE of 0.0811 USD/kWh, TLCC of 784142.00 USD, a weighted score of 0.9148. Wind power is the dominant source of power at 149.68 kW, followed by solar at 8.68 kW as a secondary contributor. The fuel cell (192.00 kW) is used sparingly as backup. Notably, the battery with a capacity of 154.21 kWh and supercapacitor at 3.10 kWh are relatively smaller as compared to those of Oluundje village, this is attributed to consistent wind availability hence reducing the dependence on energy storage. This confirms that the proposed algorithm is superior in ensuring adaptability of the HRES to local resource profiles.

Figure 6 displays the Pareto front and selected solution for Ombudiya village. It is observed from Figure 6 that the best optimal result achieves 79.82% reliability, LCOE of 0.0023 USD/kWh, and TLCC of 445091.00 USD, earning the highest weighted score of 0.8690. The configuration again places heavy reliance on biomass (100.00 kW), with moderate contributions from solar (29.01 kW) and low wind penetration (6.86 kW). A fuel cell (10.00 kW) supplements the system for rare shortfalls. Notably, the battery (40.86 kWh) and supercapacitor (0.02 kWh) capacities are adjusted to align with moderate renewable resource variability, emphasizing a balance between cost and dispatchability.

 doi:10.20944/preprints202603.1075.v1

paretofront

	LCOEkWh	TLCC	Reliability	Emissionst...	WastedPo...	CapacitieskW
	Number	Number	Number	Number	Number	Text
1	LCOE ($/kW...	TLCC ($)	Reliability	Emissions (t...	Wasted Po...	Capacities (kW)
2	0.3453	390357.00	1.28%	3015.73	38842.86	battery: 12.62, biomass: 0.00, fuel_cell: 12.00, hydrogen_budget: 13759.11, solar: 26.01, super_capacitor: 0.82, wind: 40.94
3	0.2098	419310.00	17.88%	5923.80	116162.68	battery: 168.03, biomass: 0.00, fuel_cell: 30.00, hydrogen_budget: 5867.82, solar: 60.97, super_capacitor: 3.92, wind: 13.80
4	0.3521	517190.00	37.88%	18522.84	346542.21	battery: 114.49, biomass: 0.00, fuel_cell: 18.00, hydrogen_budget: 5867.82, solar: 196.09, super_capacitor: 6.85, wind: 6.46
5	0.0015	602133.00	100.00%	90583327.86	102964.19	battery: 15.02, biomass: 200.00, fuel_cell: 30.00, hydrogen_budget: 40124.13, solar: 25.50, super_capacitor: 6.85, wind: 35.23
6	0.0042	849173.00	99.28%	45295142.08	283482.47	battery: 180.93, biomass: 100.00, fuel_cell: 60.00, hydrogen_budget: 34314.05, solar: 26.10, super_capacitor: 2.56, wind: 177.09
7	0.3008	1072327.00	56.19%	43589.68	1058227.74	battery: 102.24, biomass: 0.00, fuel_cell: 60.00, hydrogen_budget: 28912.64, solar: 447.38, super_capacitor: 2.48, wind: 110.22
8	0.0033	1307743.00	100.00%	90620993.95	1138339.64	battery: 123.11, biomass: 200.00, fuel_cell: 60.00, hydrogen_budget: 43850.88, solar: 407.34, super_capacitor: 6.85, wind: 162.43
9	0.4969	1499070.00	88.33%	43656.54	1254462.76	battery: 179.78, biomass: 0.00, fuel_cell: 48.00, hydrogen_budget: 14620.36, solar: 408.63, super_capacitor: 3.51, wind: 376.34
10	0.0084	1704141.00	99.87%	45333876.54	1410282.63	battery: 179.78, biomass: 100.00, fuel_cell: 96.00, hydrogen_budget: 67895.58, solar: 408.63, super_capacitor: 4.33, wind: 376.34
11	0.5206	647231.00	40.24%	19103.33	361281.46	battery: 113.68, biomass: 0.00, fuel_cell: 12.00, hydrogen_budget: 8086.44, solar: 190.29, super_capacitor: 9.64, wind: 87.22

(a)

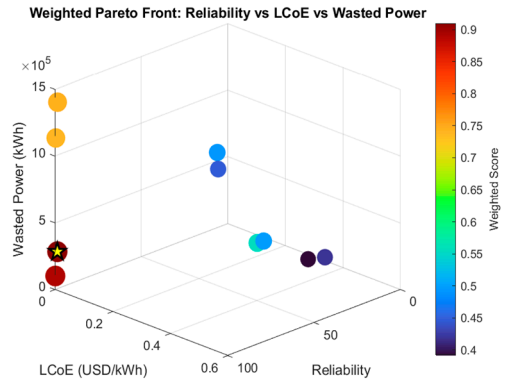

(b)

```
Results exported to ./documents/pareto_front.csv
ParetoEvaluation initialized!
Weighted Score: 0.4182, LCOE: 0.3453
Weighted Score: 0.5571, LCOE: 0.2098
Weighted Score: 0.4985, LCOE: 0.3521
Weighted Score: 0.8907, LCOE: 0.0015
Weighted Score: 0.9100, LCOE: 0.0042
Weighted Score: 0.4942, LCOE: 0.3008
Weighted Score: 0.7385, LCOE: 0.0033
Weighted Score: 0.4473, LCOE: 0.4969
Weighted Score: 0.7449, LCOE: 0.0084
Weighted Score: 0.3911, LCOE: 0.5206
```

(c)

Figure 4. Oluundje village's, (a) Pareto optimal solutions, (b) Optimal output of Reliability vs. LCOE vs. Wasted power based on weighted Pareto, and (c) Optimal Solutions based on weighted Pareto.

paretofront

	LCOEkWh	TLCC	Reliability	Emissionst...	WastedPo...	CapacitieskW
	Number	Number	Number	Number	Number	Text
1	LCOE ($/kW...	TLCC ($)	Reliability	Emissions (t...	Wasted Po...	Capacities (kW)
2	0.1193	79300.00	81.24%	416.99	12623.19	battery: 108.49, biomass: 0.00, fuel_cell: 12.00, hydrogen_budget: 43172.94, solar: 4.22, super_capacitor: 0.77, wind: 5.68
3	0.0783	122500.00	44.58%	416.99	13565.51	battery: 187.40, biomass: 0.00, fuel_cell: 30.00, hydrogen_budget: 27363.01, solar: 4.22, super_capacitor: 0.92, wind: 5.68
4	0.0328	467111.00	100.00%	3005025.41	495524.83	battery: 191.08, biomass: 100.00, fuel_cell: 24.00, hydrogen_budget: 33502.17, solar: 230.61, super_capacitor: 0.96, wind: 23.92
5	0.0811	784142.00	94.20%	2335.91	162484.52	battery: 154.21, biomass: 0.00, fuel_cell: 192.00, hydrogen_budget: 4472.54, solar: 8.68, super_capacitor: 3.10, wind: 149.64
6	0.0540	1141124.00	100.00%	3006997.79	674929.53	battery: 221.70, biomass: 100.00, fuel_cell: 162.00, hydrogen_budget: 27363.01, solar: 230.61, super_capacitor: 6.77, wind: 207.93
7	0.1095	1550400.00	100.00%	6747.63	473315.53	battery: 430.01, biomass: 0.00, fuel_cell: 282.00, hydrogen_budget: 49676.47, solar: 24.57, super_capacitor: 6.77, wind: 436.14
8	0.0589	2042141.00	100.00%	3028383.20	1192154.21	battery: 209.43, biomass: 100.00, fuel_cell: 432.00, hydrogen_budget: 44421.68, solar: 484.90, super_capacitor: 6.77, wind: 201.95
9	0.0572	2188260.00	100.00%	3028229.68	1178420.17	battery: 234.40, biomass: 100.00, fuel_cell: 504.00, hydrogen_budget: 84062.10, solar: 484.90, super_capacitor: 2.02, wind: 187.63
10	0.7370	727257.00	100.00%	48418.65	1178752.59	battery: 139.56, biomass: 0.00, fuel_cell: 18.00, hydrogen_budget: 8707.17, solar: 570.19, super_capacitor: 3.07, wind: 30.18
11	0.7658	756189.00	100.00%	48585.16	1193242.78	battery: 76.85, biomass: 0.00, fuel_cell: 18.00, hydrogen_budget: 73653.33, solar: 570.19, super_capacitor: 2.05, wind: 45.72

(a)

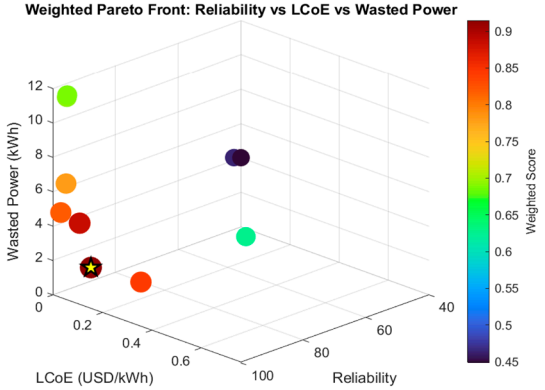

(b)

```
Results exported to ./documents/pareto_front.csv
ParetoEvaluation initialized!
Weighted Score: 0.8402, LCOE: 0.1193
Weighted Score: 0.6281, LCOE: 0.0783
Weighted Score: 0.8190, LCOE: 0.0328
Weighted Score: 0.9148, LCOE: 0.0811
Weighted Score: 0.7784, LCOE: 0.0540
Weighted Score: 0.8851, LCOE: 0.1095
Weighted Score: 0.6877, LCOE: 0.0589
Weighted Score: 0.6909, LCOE: 0.0572
Weighted Score: 0.4646, LCOE: 0.7370
Weighted Score: 0.4484, LCOE: 0.7658
```

(c)

Figure 5. Onguati village's, (a) Pareto optimal solutions, (b) Optimal output of Reliability vs. LCOE vs. Wasted power based on weighted Pareto, and (c) Optimal Solutions based on weighted Pareto.

 doi:10.20944/preprints202603.1075.v1

paretofront

	LCOEkWh	TLCC	Reliability	Emissionst...	WastedPo...	CapacitieskW
	Number	Number	Number	Number	Number	Text
1	LCOE ($/kW...	TLCC ($)	Reliability	Emissions (t...	Wasted Po...	Capacities (kW)
2	0.3922	348888.00	0.00%	2266.01	0.00	battery: 21.70, biomass: 0.00, fuel_cell: 6.00, hydrogen_budget: 1149.67, solar: 23.12, super_capacitor: 0.07, wind: 6.75
3	0.2264	395741.00	0.00%	1150.84	23044.54	battery: 16.26, biomass: 0.00, fuel_cell: 24.00, hydrogen_budget: 683.07, solar: 9.86, super_capacitor: 0.41, wind: 16.10
4	0.0023	445091.00	79.82%	45293040.91	74952.55	battery: 40.86, biomass: 100.00, fuel_cell: 6.00, hydrogen_budget: 2186.42, solar: 29.01, super_capacitor: 0.02, wind: 6.86
5	0.0026	509010.00	80.15%	45293055.29	86426.90	battery: 97.97, biomass: 100.00, fuel_cell: 24.00, hydrogen_budget: 2966.95, solar: 27.37, super_capacitor: 0.02, wind: 18.89
6	0.0999	592830.00	0.65%	742.47	29393.82	battery: 6.71, biomass: 0.00, fuel_cell: 108.00, hydrogen_budget: 3230.95, solar: 5.51, super_capacitor: 0.01, wind: 16.10
7	0.0044	874690.00	84.05%	45325762.03	884224.18	battery: 120.33, biomass: 100.00, fuel_cell: 24.00, hydrogen_budget: 3837.50, solar: 375.11, super_capacitor: 0.01, wind: 21.29
8	0.4392	1229391.00	52.49%	45277.88	1112608.91	battery: 6.19, biomass: 0.00, fuel_cell: 42.00, hydrogen_budget: 1156.04, solar: 453.23, super_capacitor: 1.90, wind: 193.18
9	0.5470	723539.00	41.66%	33341.00	633860.24	battery: 64.75, biomass: 0.00, fuel_cell: 12.00, hydrogen_budget: 407.70, solar: 352.40, super_capacitor: 0.41, wind: 16.52
10	0.5872	777844.00	41.37%	39475.17	774279.33	battery: 16.32, biomass: 0.00, fuel_cell: 12.00, hydrogen_budget: 426.43, solar: 418.86, super_capacitor: 0.13, wind: 8.61
11	0.6560	897099.00	42.63%	40367.54	812511.26	battery: 16.26, biomass: 0.00, fuel_cell: 12.00, hydrogen_budget: 460.58, solar: 418.86, super_capacitor: 0.31, wind: 72.62

(**a**)

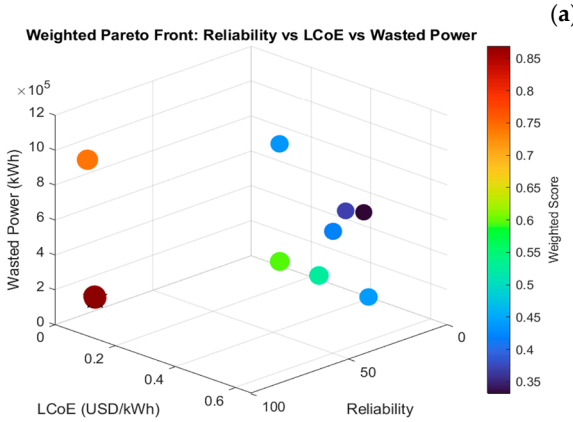

(**b**)

```
Results exported to ./documents/pareto_front.csv
ParetoEvaluation initialized!
Weighted Score: 0.4412, LCOE: 0.3922
Weighted Score: 0.5259, LCOE: 0.2264
Weighted Score: 0.8690, LCOE: 0.0023
Weighted Score: 0.8681, LCOE: 0.0026
Weighted Score: 0.5951, LCOE: 0.0999
Weighted Score: 0.7399, LCOE: 0.0044
Weighted Score: 0.4345, LCOE: 0.4392
Weighted Score: 0.4178, LCOE: 0.5470
Weighted Score: 0.3698, LCOE: 0.5872
Weighted Score: 0.3314, LCOE: 0.6560
```

(**c**)

Figure 6. Ombudiya village's, (a) Pareto optimal solutions, (b) Optimal output of Reliability vs. LCOE vs. Wasted power based on weighted Pareto, and (c) Optimal Solutions based on weighted Pareto.

(b) Seasonal Power Variations

Figure 7 illustrates the yearly variation of power and load demand on an hourly basis, while Figure 8–10 shows seasonal variations of power and load demand for the three villages.

Across all villages, solar energy emerges as the dominant source, aligning with Namibia's high solar irradiance levels. In Oluundje and Ombudiya villages, the solar resource contributes significantly during the day, between 06H00–18H00, but its variability across seasons and within days required the support from other energy sources to maintain the supply-demand balance. In Onguati village, solar energy remains significant, but it is frequently outpaced by the wind energy due to favorable wind conditions in the location (up to 20 m/s in winter). In addition, considering that wind resources are available throughout the day, it reduces the reliance on energy storage systems.

It is illustrated in Figures 7 (a)–(c) that wind energy exhibits significant variation across the case villages. Whereby wind power is minimal in Oluundje and Omudiya villages due to the prioritization of biomass resources to achieve low LCOE and LPSP. This is primarily because biomass in these areas is locally abundant, stable, and dispatchable, thereby reducing reliance on oversized energy storage systems and minimizing unmet load conditions, which in turn lowers the LPSP. Given the high biomass availability and relatively high load demand in these villages [52], wind energy contributes the least to the overall hybrid power supply. By contrast, Onguati demonstrates substantial wind power activity, especially during transitional seasons, indicating high reliance on wind due to low load demand and thus biomass is less cost effective. The dashed blue lines in Onguati village's plots as illustrated in *Figure 10* show sharp wind generation spikes, reducing the dependence on other generation sources during those periods.

Fuel cells play a pivotal role in hybrid operation, particularly in supplementing energy during shortfalls. They act as the first dispatchable backup once renewable sources (solar and wind), batteries, and supercapacitors are depleted. Their operation is prominent in all three villages, although their activity is more frequent in Oluundje and Ombudiya due to the low renewable energy surplus. Importantly, their contribution precedes biomass utilization to ensure quick-start and low-volume balancing support.

 doi:10.20944/preprints202603.1075.v1

Biomass is used primarily after the fuel cell resource becomes exhausted or insufficient, serving as the long-term

and reliable backup power source. In Oluundje and Ombudiya villages, biomass usage is dominant during the

peak evening hours and early morning hours, when solar is unavailable, and the battery's SOC is insufficient. This highlights biomass's role as a firm, and dispatchable generation asset in larger communities with high energy demand.

In this scenario, supercapacitors and batteries are utilized for short-term fluctuations and smoothing, responding to high-frequency imbalances. The plots show fast charge-discharge cycles, especially in Oluundje and Ombudiya villages, where these storage systems provide transient response support. Their contribution is minimal in terms of total energy, but essential for system stability and voltage regulation.

The load demand profile is attributed to Diurnal load shape where for residential households, peak demand is in the evening when people are home, and the lighting and heating cycles, cooking cycles and Economic and activity cycles such as School hours, market days, and work patterns shift daily.

In summary, the analysis confirms a strategic dispatch hierarchy where the renewable energy (solar and wind) is used first, followed by batteries and supercapacitors for stabilization. When deficits arise, fuel cells are engaged as the first backup due to their fast-response capability, followed by biomass generators for sustained power delivery. This staged dispatch strategy optimizes both cost and reliability, aligning with the overarching system design objectives for sustainable rural electrification in Namibia.

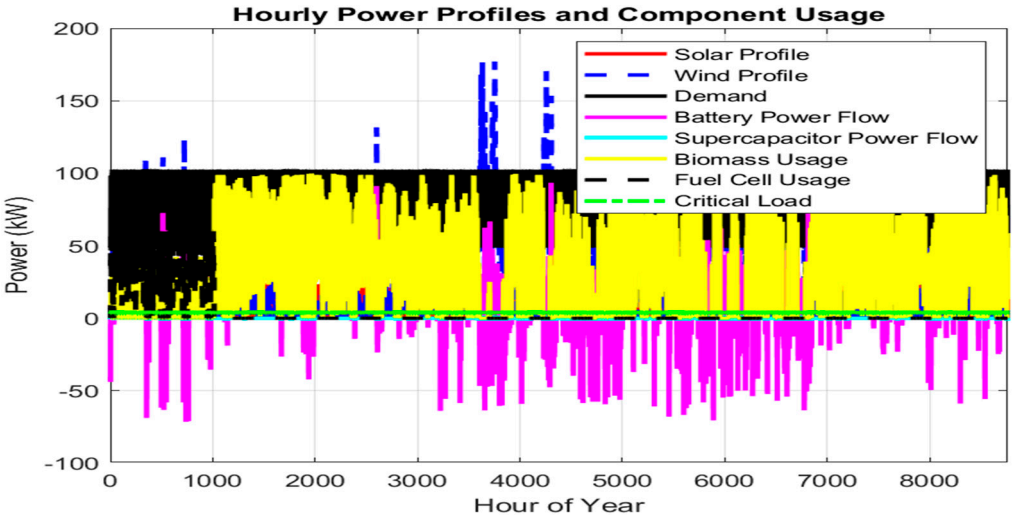

(**a**)

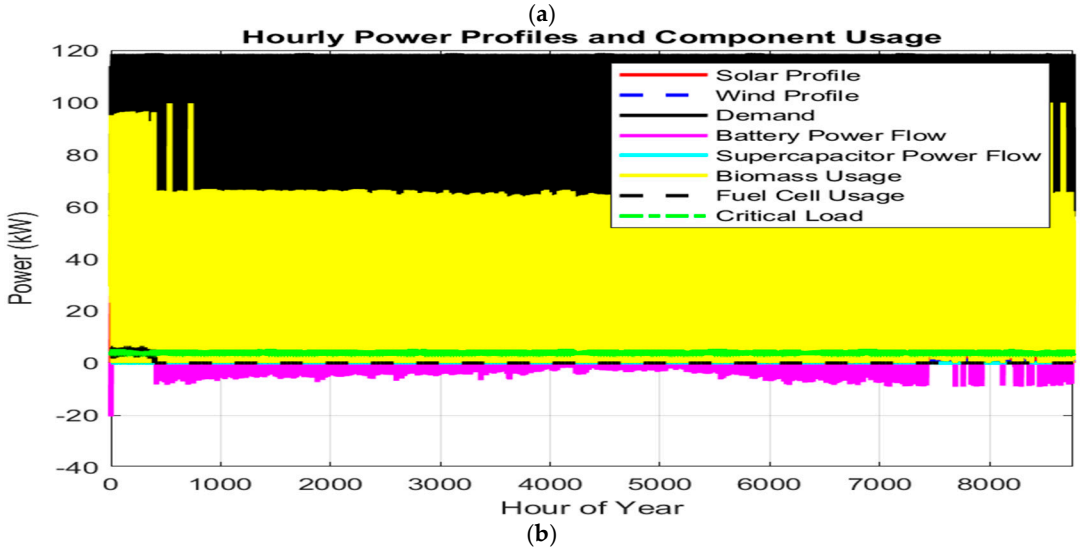

(**b**)

 doi:10.20944/preprints202603.1075.v1

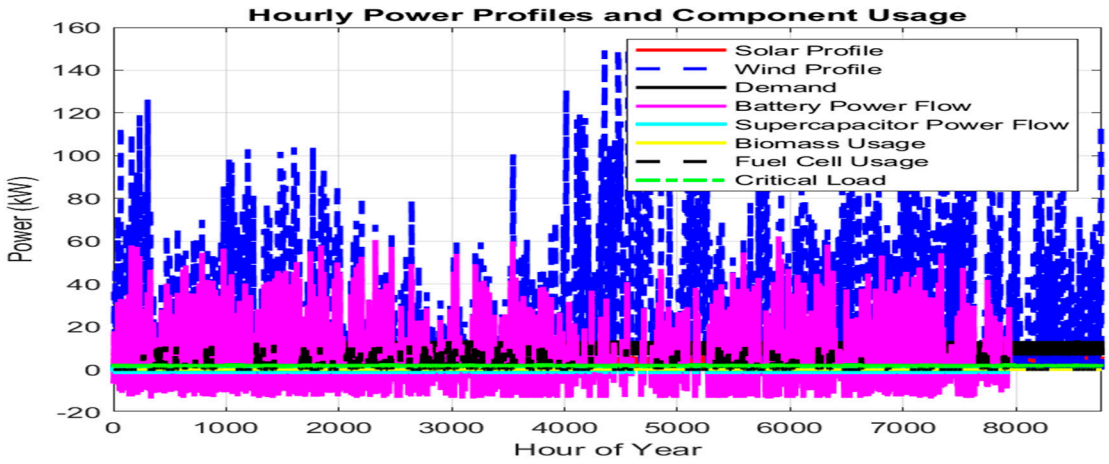

(c)

Figure 7. Hourly power profile for, (a) Oluundje, (b) Ombudiya, and (c) Onguati.

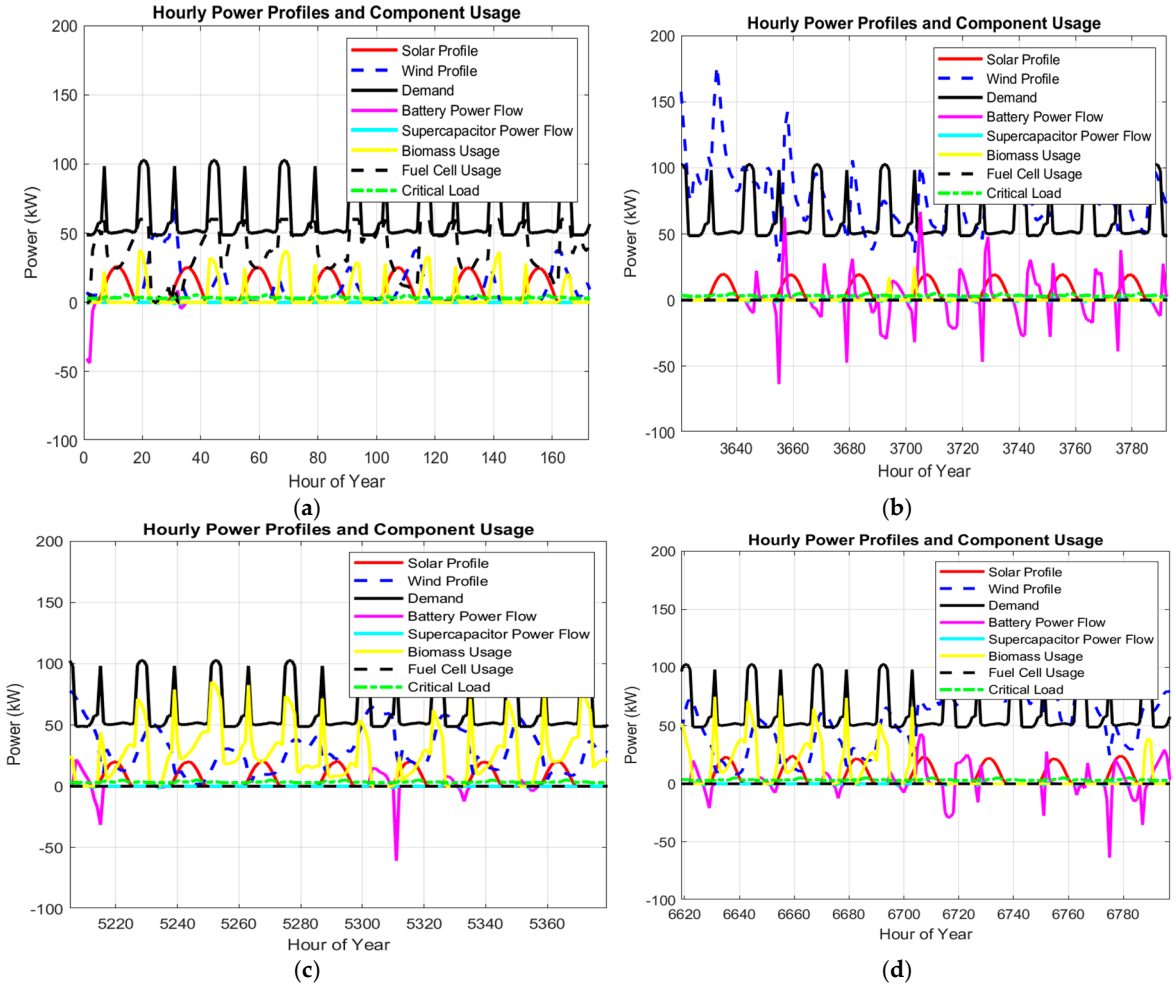

(a) (b) (c) (d)

Figure 8. Oluundje seasonal power profile (a) Summer, (b) Autumn, (c) Winter, (d) Spring.

Preprints.org (www.preprints.org) | NOT PEER-REVIEWED | Posted: 13 March 2026 doi:10.20944/preprints202603.1075.v1

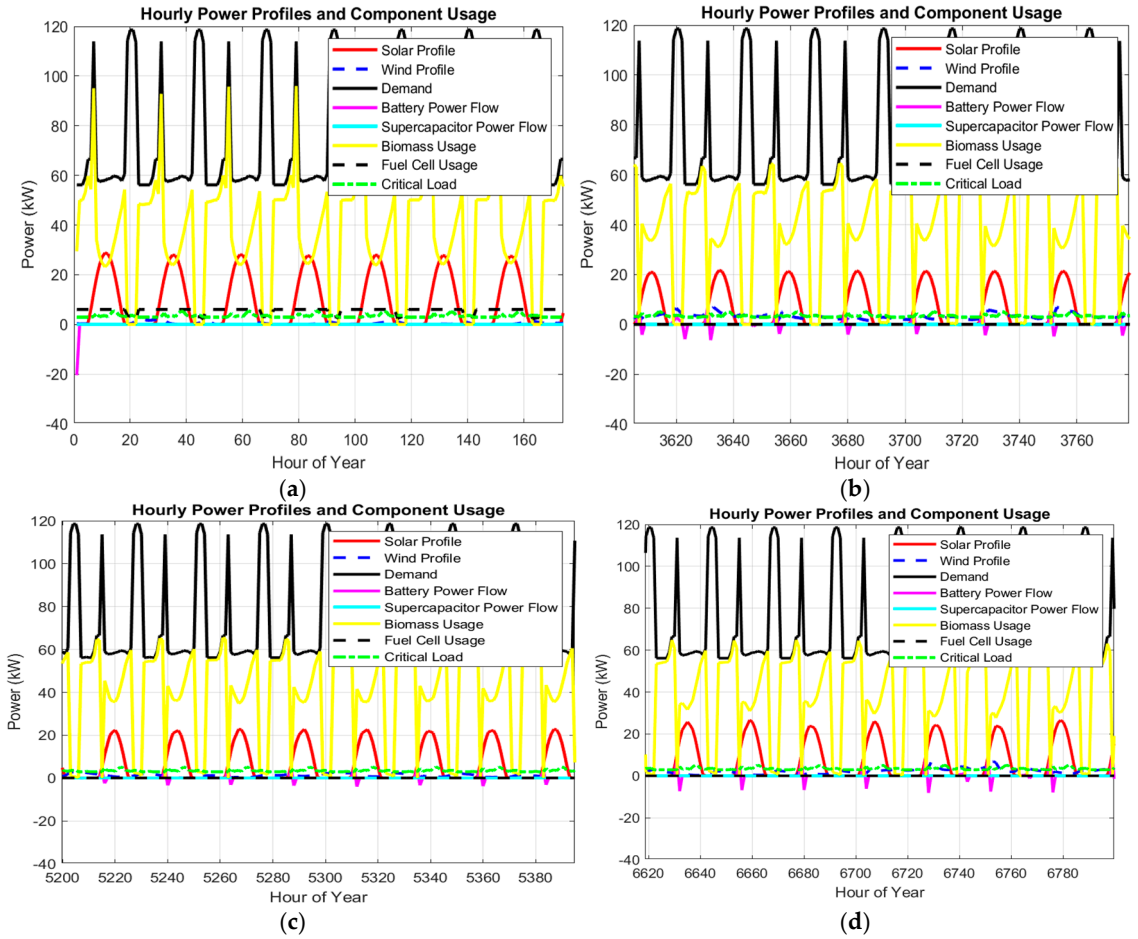

Figure 9. Ombudiya seasonal power profile, (a) Summer, (b) Autumn, (c) Winter, (d) Spring.

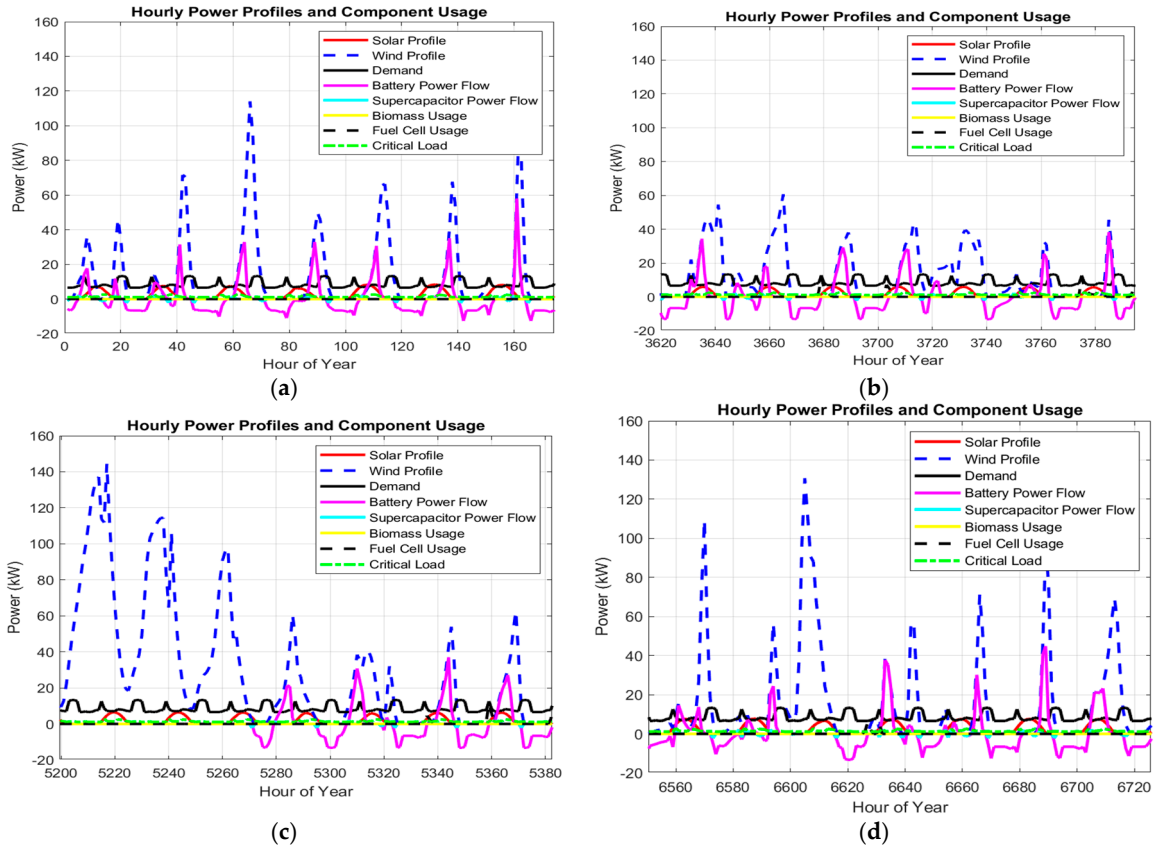

Figure 10. Onguati seasonal power profile, (a) Summer, (b) Autumn, (c) Winter, (d) Spring.

 doi:10.20944/preprints202603.1075.v1

(c) Energy Storage Flowcharts

Figures 11 to 13 present the annual behavior of dispatchable resource capacities and energy storage in the optimized hybrid energy systems for Oluundje, Ombudiya, and Onguati villages. This includes the remaining fuel budgets (in kWh) for fuel cells and biomass generators, as well as the State of Charge (SOC) trends for batteries and supercapacitors throughout the year.

As shown in Figures 11 and 12, there is a steady depletion of the available hydrogen storage allocated to the fuel cell before biomass activation in Oluundje and Ombudiya villages, respectively, consistent with the dispatch strategy where fuel cells act as the primary dispatchable source when RESs are insufficient. Biomass is engaged after the energy in fuel cells gets depleted to supply the remaining unmet load. This layered approach reflects both economic and operational priorities; prioritizing hydrogen utilization before biomass due to emissions and operational cost considerations. The SOC levels of the battery and supercapacitors in these villages remain relatively stable, generally above 20% and below 80% and 90% for the battery and supercapacitor, respectively, and there is minimal usage. These storage devices are mainly used for short-term balancing and transient support rather than continuous cycling. By prioritizing dispatchable generation (fuel cell and biomass) over prolonged storage discharge, the algorithm mitigates excessive cycling stress, reduces

degradation rates, and extends storage lifespan. Consequently, storage devices function mainly as dynamic stabilizers for power smoothing and rapid response support, rather than as continuous energy sources.

In Onguati village, biomass resource remains virtually untapped throughout the year, as evidenced by the flat energy budget curve in Figure 13(a). This occurs because wind power, which serves as the village's primary energy source, is sufficient to meet most of the load demand, while the fuel cell provides reliable backup during renewable shortfalls. Given the relatively low load demand and substantial wind availability, the optimization algorithm identifies biomass generation as uneconomical, since activating it would increase operational costs and emissions without significantly improving reliability. These results confirm that wind power can meet most of the load when supplemented by the fuel cell, battery, and supercapacitors. However, repeated SOC cycling observed in Onguati village's storage systems (battery and supercapacitor) highlights their critical role in mitigating wind intermittency and managing short-term power fluctuations.

The variation in storage usage patterns across villages underscores the importance of site-specific hybrid energy system planning. While Oluundje and Ombudiya villages depend significantly on dispatchable resources to meet the load, Onguati village's system capitalizes on wind abundance, relying more on battery and supercapacitor and fuel cell than on biomass-based generation.

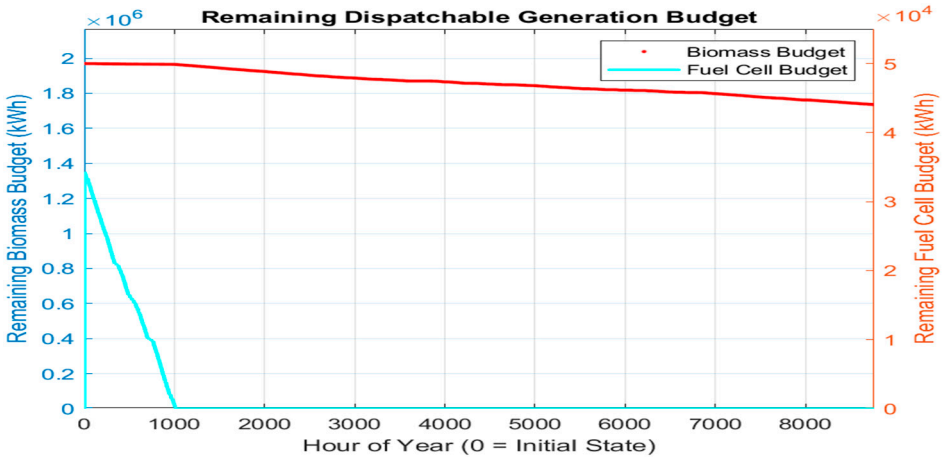

(**a**)

 doi:10.20944/preprints202603.1075.v1

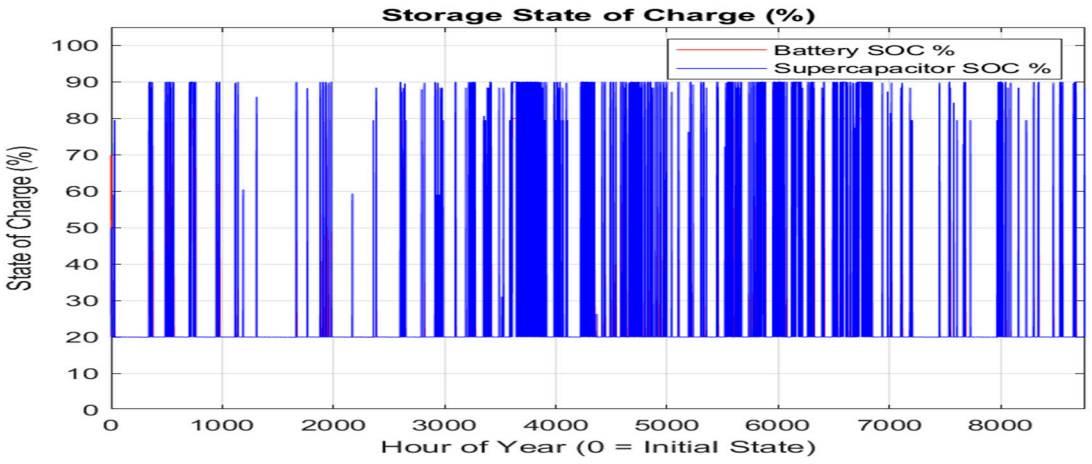

(**b**)

Figure 11. Oluundje village's, (a) Available dispatchable capacity, (b) Battery and Supercapacitor SOC (%).

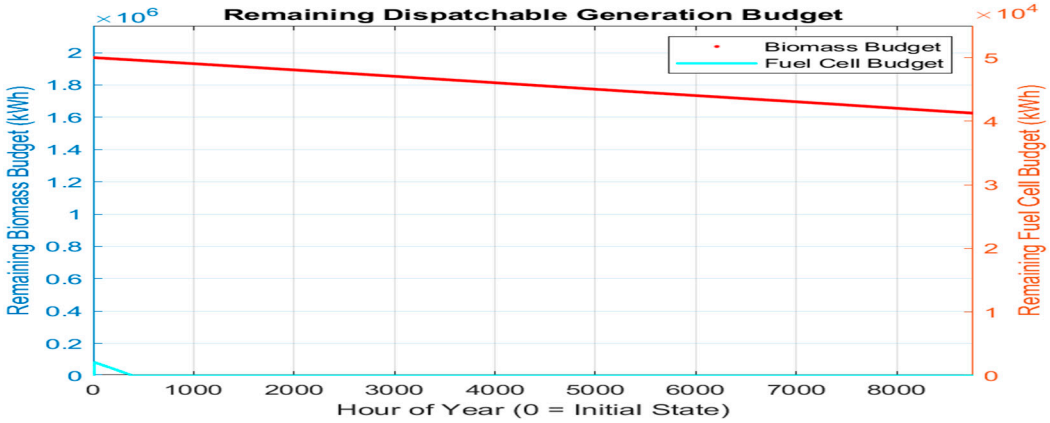

(**a**)

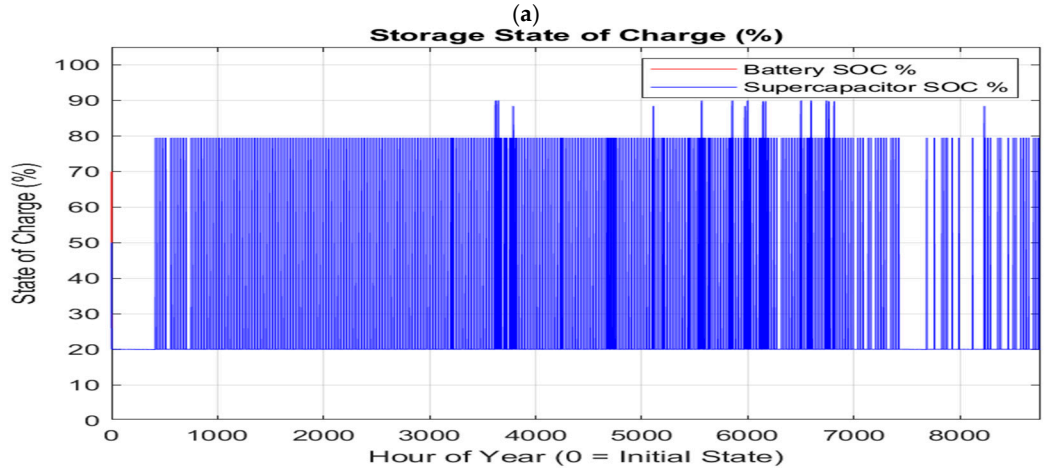

(**b**)

Figure 12. Ombudiya village's, (a) Available dispatchable capacity, (b) Battery and Supercapacitor SOC (%).

 doi:10.20944/preprints202603.1075.v1

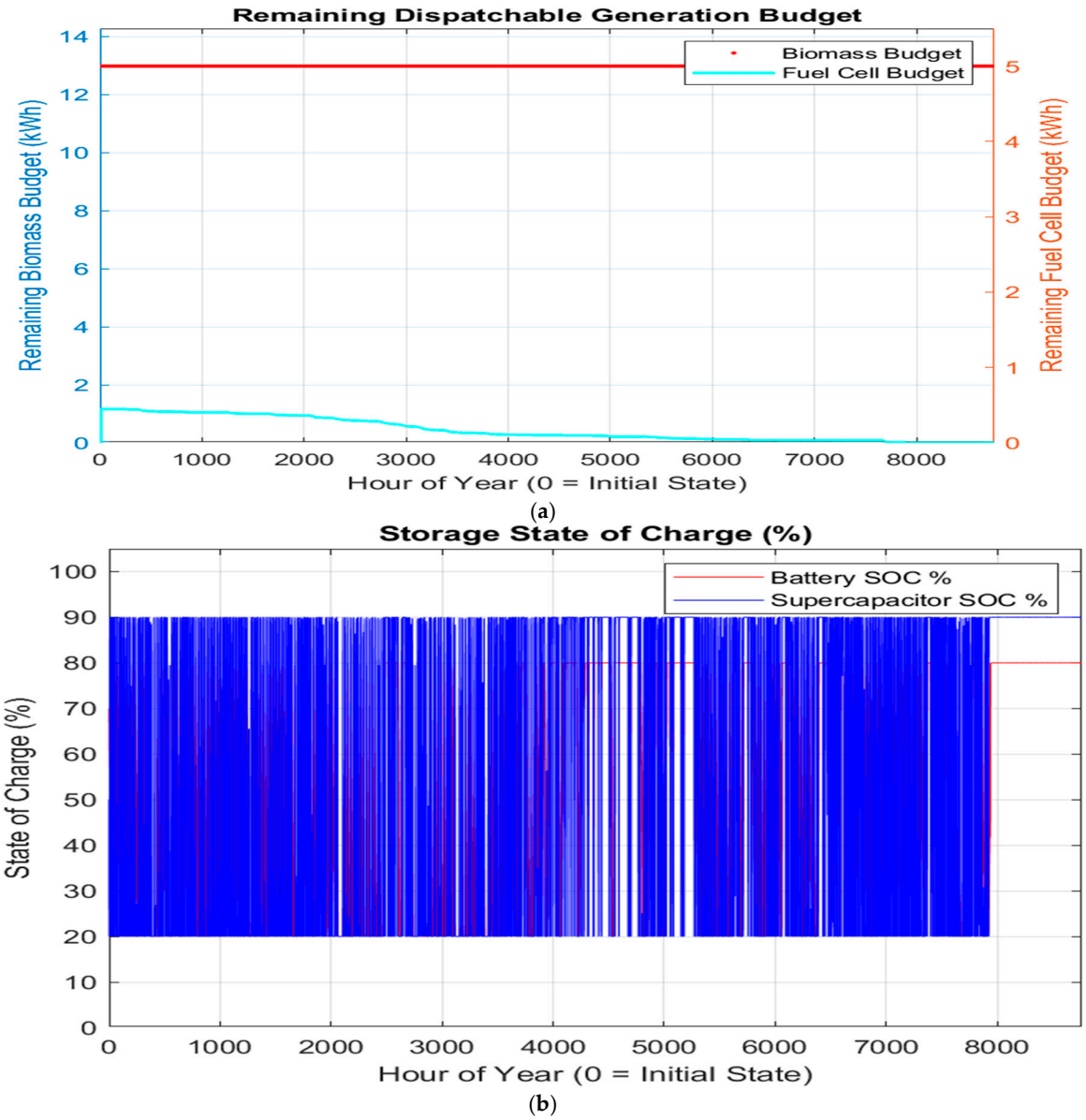

Figure 13. Onguati village's, (a) Available dispatchable capacity, (b) Battery and Supercapacitor SOC (%).

(d) Capacity Factors of Energy Sources

Figure 14 illustrates the annual capacity factors (CF) of solar, wind, biomass, and fuel cell systems for the 3 villages. The results indicate that solar PV consistently exhibits the highest CF across all three locations, ranging from approximately 23% to 27%. This reflects not only the abundant solar resource potential in Namibia's semi-arid climate but also the low seasonal variability, high solar irradiance levels, and favorable temperature conditions that enhance PV conversion efficiency. In addition, the optimization algorithm prioritizes solar generation due to its zero-fuel cost, low operational expenditure, and high reliability, leading to consistently high utilization throughout the year and as a cornerstone of HRESs.

In contrast, wind energy displays relatively lower CF values, typically below 14%, suggesting limited or inconsistent wind availability in the regions studied. This positions wind as a supplementary energy source, particularly useful for covering night-time or seasonal gaps in solar power generation.

Biomass-based systems achieve notably high CF in Oluundje and Ombudiya villages, ranging from 25% to 30%, signifying effective utilization of available feedstock and efficient integration of biomass generation into the dispatch strategy. Conversely, Onguati village exhibits zero CF for

 doi:10.20944/preprints202603.1075.v1

biomass systems. This is attributed to lower demand levels, and resource constraints, considering that the configuration is optimized around wind energy.

The fuel cell CF remains the lowest across all villages, ranging between 3% and 6%. This is due to minimal periods of concurrent renewable energy shortfalls where fuel cells were to be used as a back-up source of power as well as considering the fuel limitations. The observed differences in CF values across different technologies and locations underscore the necessity for site-specific resource assessment and hybrid system optimization to ensure both technical reliability and economic feasibility.

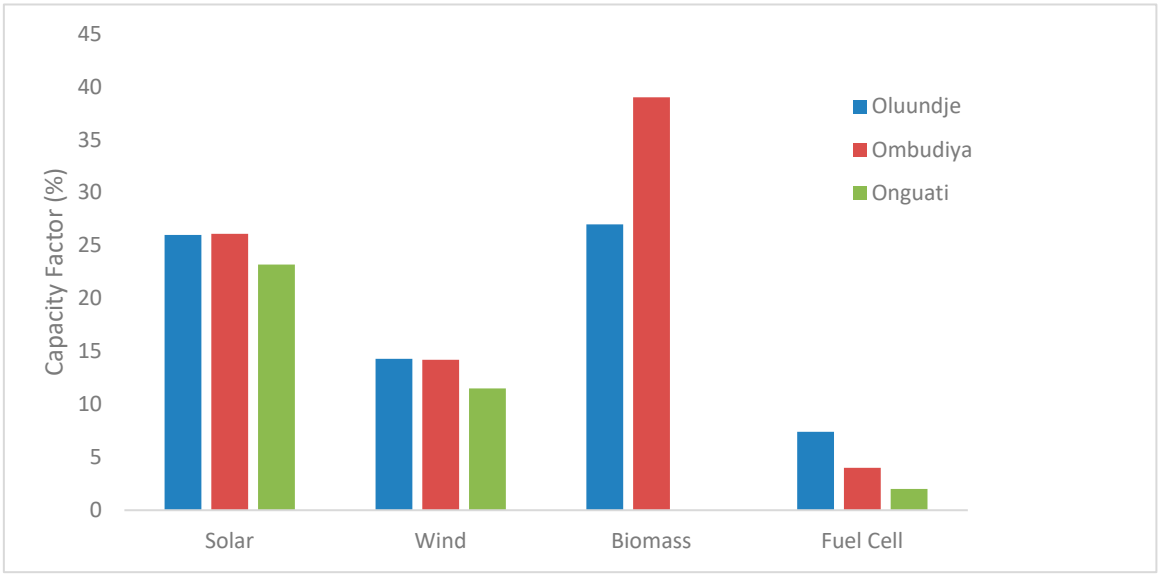

Figure 14. Capacity Factors for the different energy sources for the 3 villages.

(e) Composition of the Energy Sources

Figure 15 illustrates the optimal combination of the energy mix for the 3 villages under consideration. It can be shown that wind energy is the dominant source in Onguati village, driven by a favorable and consistently available wind resource (up to 20 m/s in winter). By contrast, biomass accounts for the majority of energy supply in Ombudiya and Oluundje villages, reflecting the availability of sustainable biomass feedstock and the higher energy demand in the 2 villages with higher communities.

The prominence of biomass in Ombudiya and Oluundje villages aligns with the findings in [51]. It is observed from Figure 15 that solar PV contributes a comparatively equal power in all the 3 villages, but its share remains moderate due to its intermittency, limited generation during nighttime, and optimized sizing constraints aimed at minimizing costs. Fuel cells, powered by stored hydrogen, contribute the least across all cases and are only dispatched under circumstances when renewable generation sources are insufficient.

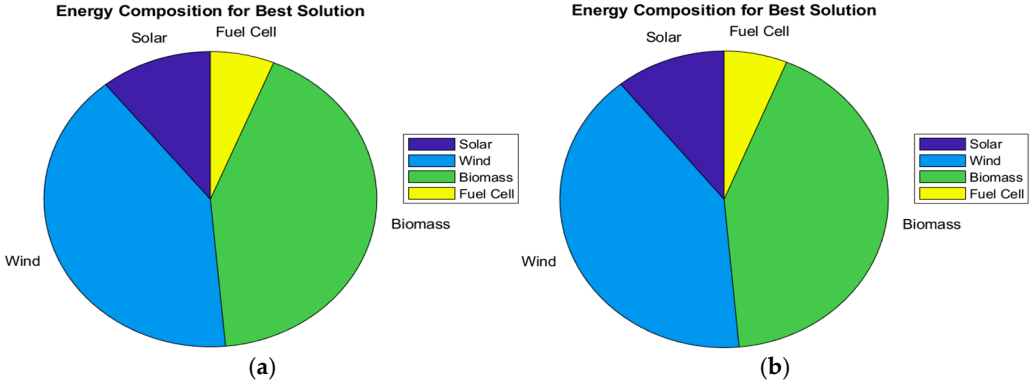

 doi:10.20944/preprints202603.1075.v1

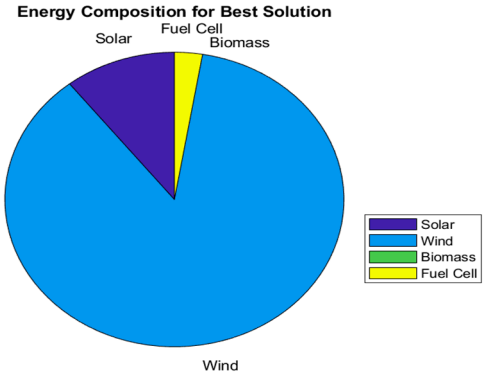

(**c**)

Figure 15. Energy sources' composition for (a) Oluundje, (b) Ombudiya, (c) Onguati.

These findings emphasize the importance of site-specific system configuration that accounts for local renewable resource availability, population-based demand patterns, and cost-effectiveness in resource utilization. Tailoring the HRES design in this manner enhances system reliability, ensures cost-efficiency, and promotes sustainable rural electrification. The results from the optimization further confirm that multi-objective NSGA-II is effective in designing HRES for enhanced rural electrification. Each village's best optimal solution varied depending on their load profiles and resource availability. Key takeaways include the importance of dispatchable sources like biomass and fuel cells for reliability, the role of supercapacitors in transient stability, and the use of hydrogen storage for long-duration support. The framework developed here can be scaled and adapted for other rural locations in Namibia and beyond.

Furthermore, the graphical and analytical results obtained for three villages collectively illustrate the development of the adaptable hybrid renewable energy framework capable of replication across diverse rural contexts in Namibia. The resource assessment graphs (Figure 1–Figure 2) and Table 2 revealed significant spatial and temporal variations in wind speed, solar irradiance across the three sites, and biomass availability, forming the foundation for location-specific parameterization within the model.

The optimization results, including the Pareto fronts and reliability-LCOE-wasted power trade-off plots (Figure 4–Figure 6) demonstrated that the model dynamically adjusted the optimal configuration of solar PV, wind turbines, biomass generators, and hydrogen-based fuel cell systems according to each village's resource potential and demand profile. For instance, the Pareto front for Onguati village favoured a solar–wind–fuel cell hybrid system due to the high solar insolation and wind resources and moderate biomass potential and low load demand. Conversely, Oluundje and Ombudiya villages' optimal solution incorporated more biomass capacity owing to higher biomass resources, and load demand due to huge community size making it more cost effective. The available dispatch capacity and state-of-charge (SOC) plots (Figure 11–Figure 13) validated the control strategy's effectiveness in maintaining system stability and ensuring a balanced power sharing among the battery, supercapacitor, and hydrogen storage subsystems as well as biomass resources availability.

Furthermore, the reliability and sensitivity analyses confirmed that the framework consistently achieved system reliability above 75% while maintaining competitive LCOE values between $0.0023 and $0.0811/kWh, outperforming existing diesel mini-grids such as those in Tsumkwe and Gam locations. These results collectively verify that the framework can automatically adapt to varying technical, economic, and resource constraints. By updating the input datasets, such as local renewable resource profiles, and load patterns, the same optimization simulation framework can be applied to any other rural area in Namibia to design a site-specific, reliable, and economically viable hybrid energy system, thus promoting replicable, scalable and sustainable rural electrification.

 doi:10.20944/preprints202603.1075.v1

The findings in this section demonstrate that integrating multiple renewable sources with appropriate storage systems can effectively enhance the reliability and affordability of rural electrification. Seasonal analyses confirmed that hybrid configurations outperform single-resource systems in terms of stability and energy availability. The Pareto-optimal results underscore the balance between cost and reliability, supporting sustainable energy planning decisions. These results validate the robustness of the proposed optimization framework. The concluding section summarizes the research contributions and provides recommendations for future work.

3. Conclusions

An optimization model of Hybrid Renewable Energy Sources and Storage Systems was developed and evaluated in this research study to address the challenge of sustainable rural electrification in Namibia. The proposed model integrated solar, wind, and biomass renewable sources with a hybrid energy storage system comprising batteries, supercapacitors, and hydrogen-based fuel cells. The study was grounded in the real-world context of Namibia's rural energy access challenges and emphasized technical, economic, and environmental performance metrics through multi-objective optimization.

Through a multi-objective optimization framework, the model simultaneously minimized Total Life Cycle Cost (TLCC), Levelized Cost of Electricity (LCOE), and excess energy generation, while maximizing system reliability and renewable energy utilization. Simulations were conducted for three distinct rural sites in Namibia, using real-world renewable resource data, technical constraints, and context-specific load forecasts. The optimized configurations maximized energy demand coverage, minimized critical load shortfalls, and maintained high power quality, all while remaining within acceptable economic thresholds.

In comparative analyses, the proposed algorithm consistently outperformed existing models such as standard HOMER-based optimizations in terms of economic feasibility, dispatch reliability, and energy efficiency. Notably, the integration of supercapacitors for dynamic load balancing and hydrogen storage for long-duration autonomy allowed the system to achieve superior resilience against renewable intermittency, an area where conventional battery-only or single-source designs often fail.

In general, the following was observed from the study:

- Solar PV emerged as the dominant energy source due to its abundance and cost-efficiency, contributing the overall highest share of energy supply across all study areas.
- Wind energy served as a valuable complementary resource, especially during night and non-solar periods, improving the load-following capability of the Hybrid Renewable Energy System (HRES).
- Biomass generators contributed dispatchable power during seasonal shortfalls and extended low-renewable periods but required careful fuel budgeting to avoid oversizing and unsustainable costs.
- Batteries provided daily cycling capabilities, while supercapacitors effectively responded to high-frequency renewable resources and load fluctuations and reduced stress on the batteries.
- The hydrogen-based fuel cell was critical for maintaining supply reliability during prolonged renewable generation deficits, particularly during seasonal lows, albeit at a higher operational cost.
- The best optimal HRES configurations achieved high system reliability (>75%) while maintaining highly competitive LCOE values between $0.0023–$0.0811/kWh, significantly outperforming both existing diesel mini-grids such as Tsumkwe (≈ $0.55/kWh) and Gam (≈ $0.91/kWh) [53], as well as Namibia's average grid electricity cost of approximately $0.134/kWh [54]. This demonstrates the superior techno-economic viability of renewable-based hybrid systems for rural electrification. Such cost advantages, coupled with improved reliability and environmental sustainability, position HRES as a long-term substitute for fossil-

 doi:10.20944/preprints202603.1075.v1

fuel-based and grid-dependent systems, requiring only minimal institutional support to accelerate large-scale deployment across off-grid regions.

- Storage hybridization (Battery + Supercapacitor + Hydrogen Tank) resulted in improved cost-effectiveness, longevity of components, and operational stability of the system.
- Excess energy was minimized in most scenarios due to optimal component sizing and intelligent dispatch logic embedded in the simulation framework.
- Trade-offs were observed between cost and reliability, were higher reliability generally required increased storage sizing, especially hydrogen and fuel cell dependence, leading to increased TLCC.
- The model proved scalable and replicable, with successful validation in three distinct rural contexts, indicating its adaptability for national rural electrification planning.
- The framework also incorporated Namibia-specific socio-economic conditions, such as affordability thresholds (electricity cost ≤ 5% of household income), ensuring realistic and inclusive system

References

1. B. Hachim, D. Dahlioui, and A. Barhdadi, "Electrification of rural and arid areas by solar energy applications case study: Boumhaout village in south of Morocco," *Proc. 2018 6th Int. Renew. Sustain. Energy Conf. IRSEC 2018*, Jul. 2018, doi: 10.1109/IRSEC.2018.8702978.
2. V. Saini, S.K. Singal, and R. P. Saini, "Renewable energy-based system for electrification of remote villages," *2022 Int. Conf. Green Energy, Comput. Sustain. Technol. GECOST 2022*, pp. 6–10, 2022, doi: 10.1109/GECOST55694.2022.10010609.
3. "Access to electricity (% of population) | Data." Accessed: Aug. 14, 2025. [Online]. Available: https://data.worldbank.org/indicator/eg.elc.accs.zs
4. NamPower (Pty) Ltd., "NamPower Integrated Annual Report 2024," Windhoek, 2024. [Online]. Available: https://www.nampower.com.na/public/docs/annual-reports/NamPower_Integrated_Annual_Report_2024.pdf
5. A. M. Patel and S. K. Singal, "Implementation Methodology of Integrated Renewable Energy System Modeling for Off-grid Rural Electrification: A review," *Proc. Conf. Ind. Commer. Use Energy, ICUE*, vol. 2018-October, Jul. 2018, doi: 10.23919/ICUE-GESD.2018.8635707.
6. Y. Zahraoui et al., "Energy Management System in Microgrids: A Comprehensive Review," *Sustain. 2021, Vol. 13, Page 10492*, vol. 13, no. 19, p. 10492, Sep. 2021, doi: 10.3390/SU131910492.
7. A. Z. AL Shaqsi, K. Sopian, and A. Al-Hinai, "Review of energy storage services, applications, limitations, and benefits," *Energy Reports*, vol. 6, pp. 288–306, Dec. 2020, doi: 10.1016/J.EGYR.2020.07.028.
8. A. Alzahrani, S.K. Ramu, G. Devarajan, I. Vairavasundaram, and S. Vairavasundaram, "A Review on Hydrogen-Based Hybrid Microgrid System: Topologies for Hydrogen Energy Storage, Integration, and Energy Management with Solar and Wind Energy," *Energies*, vol. 15, no. 21, Nov. 2022, doi: 10.3390/EN15217979.
9. X. Liu, T. Zhao, H. Deng, P. Wang, J. Liu, and F. Blaabjerg, "Microgrid Energy Management with Energy Storage Systems: A Review," *CSEE J. Power Energy Syst.*, vol. 9, no. 2, pp. 483–504, Mar. 2023, doi: 10.17775/CSEEJPES.2022.04290.
10. S. Keller, S. Naciri, A. Nejmi, and J. Dos Ghali, "Simulation-based decision support tool for electrification of isolated areas using a network with multiple renewable sources," *2007 Int. Conf. Clean Electr. Power, ICCEP '07*, pp. 1–8, 2007, doi: 10.1109/ICCEP.2007.384177.
11. C. Gusain, M. Mohan Tripathi, and U. Nangia, "Study of Meta-heuristic Optimization Methodologies for Design of Hybrid Renewable Energy Systems," *Therm. Sci. Eng. Prog.*, vol. 39, p. 101711, Mar. 2023, doi: 10.1016/J.TSEP.2023.101711.
12. B. Akbas, A.S. Kocaman, D. Nock, and P. A. Trotter, "Rural electrification: An overview of optimization methods," *Renew. Sustain. Energy Rev.*, vol. 156, p. 111935, Mar. 2022, doi: 10.1016/J.RSER.2021.111935.

 doi:10.20944/preprints202603.1075.v1

13. A. F. Bastos and R. D. Trevizan, "Feasibility of 100% Renewable-Energy-Powered Microgrids Serving Remote Communities," *2023 IEEE Power Energy Soc. Innov. Smart Grid Technol. Conf. ISGT 2023*, 2023, doi: 10.1109/ISGT51731.2023.10066456.
14. M. S. Javed, A. Song, and T. Ma, "Techno-economic assessment of a stand-alone hybrid solar-wind-battery system for a remote island using genetic algorithm," *Energy*, vol. 176, pp. 704–717, Jun. 2019, doi: 10.1016/J.ENERGY.2019.03.131.
15. F. Canziani, R. Vargas, and J. A. Gastelo-Roque, "Hybrid Photovoltaic-Wind Microgrid With Battery Storage for Rural Electrification: A Case Study in Perú," *Front. Energy Res.*, vol. 8, p. 528571, Feb. 2021, doi: 10.3389/FENRG.2020.528571/BIBTEX.
16. C. Melkia, S. Ghoudlburk, Y. Soufi, M. Maamri, and M. Bayoud, "Battery-Supercapacitor Hybrid Energy Storage Systems for Stand-Alone Photovoltaic," *Rev. des Compos. des Mater. Av.*, vol. 24, no. 5–6, pp. 265–271, 2022, doi: 10.18280/EJEE.245-605.
17. S. Ferahtia, A. Djerioui, S. Zeghlache, and A. Houari, "A hybrid power system based on fuel cell, photovoltaic source and supercapacitor," *SN Appl. Sci.*, vol. 2, no. 5, pp. 1–11, May 2020, doi: 10.1007/S42452-020-2709-0/FIGURES/15.
18. G. Prinsloo, R. Dobson, and A. Mammoli, "Smart Village Load Planning Simulations in Support of Digital Energy Management for Off-grid Rural Community Microgrids," *Curr. Altern. Energy*, vol. 2, no. 1, pp. 2–18, Nov. 2017, doi: 10.2174/2405463102666171122161858.
19. S. Kühnel et al., "Holistic approach to develop electricity load profiles for rural off-grid communities in sub-Saharan Africa," *Proc.—ISES Sol. World Congr. 2021*, pp. 348–361, 2021, doi: 10.18086/SWC.2021.20.02.
20. J. Namaganda-Kiyimba, J. Mutale, and B. Azzopardi, "Improving the Load Estimation Process in the Design of Rural Electrification Systems," *Energies 2021, Vol. 14, Page 5505*, vol. 14, no. 17, p. 5505, Sep. 2021, doi: 10.3390/EN14175505.
21. R. Takalani and B. Bekker, "Load and load growth models for rural microgrids, and how to future-proof designs," *2020 Int. SAUPEC/RobMech/PRASA Conf. SAUPEC/RobMech/PRASA 2020*, Jan. 2020, doi: 10.1109/SAUPEC/ROBMECH/PRASA48453.2020.9041001.
22. A. M. Patel and S. K. Singal, "Renewable Energy Source based Hybrid Power Generation Scheme for Off-grid Rural Electrification," *2017 14th IEEE India Counc. Int. Conf. INDICON 2017*, Oct. 2018, doi: 10.1109/INDICON.2017.8487807.
23. E. Hamatwi, C. Nyirenda, and I. Davidson, "Optimisation of a Hybrid PV-Diesel System for Rural Application: The Case of Oluundje Village, Namibia Optimisation of a Hybrid PV-Diesel System," vol. 9, pp. 9–25, 2017.
24. T. Wanjekeche and T. Ananias, "Optimal and Economic Evaluation of a Stand-alone Microgrid for Electricity and Water Supply for Namibia's Rural Village," *Am. J. Energy Eng. 2019, Vol. 7, Page 64*, vol. 7, no. 3, pp. 64–73, Nov. 2019, doi: 10.11648/J.AJEE.20190703.12.
25. A. Mohammad-Alikhani, A. Mahmoudi, and S. Kahourzade, "Multi-objective optimization of system configuration and component capacity in AC mini-grid hybrid power system," *9th IEEE Int. Conf. Power Electron. Drives Energy Syst. PEDES 2020*, Dec. 2020, doi: 10.1109/PEDES49360.2020.9379526.
26. E. I. Come Zebra, H.J. van der Windt, G. Nhumaio, and A. P. C. Faaij, "A review of hybrid renewable energy systems in mini-grids for off-grid electrification in developing countries," *Renew. Sustain. Energy Rev.*, vol. 144, p. 111036, Jul. 2021, doi: 10.1016/J.RSER.2021.111036.
27. N. Amir, D.N. Purnamasari, and F. A. Mufarroha, "Application of Renewable Energy Sources for Rural Electrification at a Remote Outer Island," *Proc.—2021 IEEE 7th Inf. Technol. Int. Semin. ITIS 2021*, 2021, doi: 10.1109/ITIS53497.2021.9791801.
28. R. F. Dad and S. Saleem, "A Comparative Study of Various Optimization Techniques to Size a Hybrid Renewable Energy System," *2022 24th Int. Multitopic Conf. INMIC 2022*, 2022, doi: 10.1109/INMIC56986.2022.9972951.
29. A. H. Slama, M. Saidi, and L. Saidi, "Optimal Sizing for Renewable Hybrid Energy Systems: A Review With Some Applications," *2022 IEEE Int. Conf. Electr. Sci. Technol. Maghreb, Cist. 2022*, 2022, doi: 10.1109/CISTEM55808.2022.10043975.

 doi:10.20944/preprints202603.1075.v1

30. H. Nabipour-Afrouzi, S.H. Wen Yii, J. Ahmad, and M. Tabassum, "Comprehensive review on appropriate sizing and optimization technique of hybrid PV-wind system," *Asia-Pacific Power Energy Eng. Conf. APPEEC*, vol. 2018-October, pp. 364–369, Dec. 2018, doi: 10.1109/APPEEC.2018.8566269.
31. M. Thirunavukkarasu, Y. Sawle, and H. Lala, "A comprehensive review on optimization of hybrid renewable energy systems using various optimization techniques," *Renew. Sustain. Energy Rev.*, vol. 176, p. 113192, Apr. 2023, doi: 10.1016/J.RSER.2023.113192.
32. A. Maheri, "MOHRES, a Software Tool for Analysis and Multiobjective Optimisation of Hybrid Renewable Energy Systems-An Overview of Capabilities," *Proc. 2021 6th Int. Symp. Environ. Energies Appl. EFEA 2021*, Mar. 2021, doi: 10.1109/EFEA49713.2021.9406221.
33. S. Husain and N. A. Shrivastava, "A Comparative Analysis of Multi-objective Optimization Algorithms for Stand-Alone Hybrid Renewable Energy System," *2nd Int. Conf. Innov. Mech. Ind. Appl. ICIMIA 2020—Conf. Proc.*, pp. 255–260, Mar. 2020, doi: 10.1109/ICIMIA48430.2020.9074903.
34. M. I. Hlal et al., "NSGA-II and MOPSO based optimization for sizing of hybrid PV/wind/battery energy storage system Cost of energy Hybrid renewable energy system Loss of power supply probability MOPSO Multi objectives NSGA_II," *Int. J. Power Electron. Drive Syst.*, vol. 10, no. 1, pp. 463–478, 2019, doi: 10.11591/ijpeds.v10.i1.pp463-478.
35. X. Zhu, P. Gui, X. Zhang, Z. Han, and Y. Li, "Multi-objective optimization of a hybrid energy system integrated with solar-wind-PEMFC and energy storage," *J. Energy Storage*, vol. 72, Nov. 2023, doi: 10.1016/J.EST.2023.108562.
36. S. Feleke, D. Anteneh, B. Pydi, R. Satish, A. El-Shahat, and A. Y. Abdelaziz, "Feasibility and Potential Assessment of Solar Resources: A Case Study in North Shewa Zone, Amhara, Ethiopia," *Energies*, vol. 16, no. 6, Mar. 2023, doi: 10.3390/EN16062681.
37. T. N. Rateele and L. Z. Thamae, "An optimization approach for the economic dispatch incorporating renewable energy resources into Lesotho power sources portfolio," *Heliyon*, vol. 9, no. 4, p. e14748, Apr. 2023, doi: 10.1016/J.HELIYON.2023.E14748.
38. A. Jain, P. Das, S. Yamujala, R. Bhakar, and J. Mathur, "Resource potential and variability assessment of solar and wind energy in India," *Energy*, vol. 211, p. 118993, Nov. 2020, doi: 10.1016/J.ENERGY.2020.118993.
39. A. Askarzadeh and L. dos Santos Coelho, "A novel framework for optimization of a grid independent hybrid renewable energy system: A case study of Iran," *Sol. Energy*, vol. 112, pp. 383–396, Feb. 2015, doi: 10.1016/J.SOLENER.2014.12.013.
40. K. Gebrehiwot, M.A.H. Mondal, C. Ringler, and A. G. Gebremeskel, "Optimization and cost-benefit assessment of hybrid power systems for off-grid rural electrification in Ethiopia," Energy, vol. 177, pp. 234–246, 2019, doi: 10.1016/j.energy.2019.04.095
41. S. Rajanna and R. P. Saini, "Optimal modeling of an integrated renewable energy system with battery storage for off grid electrification of remote rural area," *1st IEEE Int. Conf. Power Electron. Intell. Control Energy Syst. ICPEICES 2016*, Feb. 2017, doi: 10.1109/ICPEICES.2016.7853114.
42. O. O. Akinte, B. Plangklang, B. Prasartkaew, and T. S. Aina, "Energy Storage Management of a Solar Photovoltaic–Biomass Hybrid Power System," *Energies 2023, Vol. 16, Page 5122*, vol. 16, no. 13, p. 5122, Jul. 2023, doi: 10.3390/EN16135122.
43. R. R. Thakkar and R. R. Thakkar, "Electrical Equivalent Circuit Models of Lithium-ion Battery," *Manag. Appl. Energy Storage Devices*, Sep. 2021, doi: 10.5772/INTECHOPEN.99851.
44. F. Naseri, S. Karimi, E. Farjah, and E. Schaltz, "Supercapacitor management system: A comprehensive review of modeling, estimation, balancing, and protection techniques," *Renew. Sustain. Energy Rev.*, vol. 155, p. 111913, Mar. 2022, doi: 10.1016/J.RSER.2021.111913.
45. A. hamlat, M. 'hamed sekour, M. mankour, M. yahiaoui, M. khalfaoui, and B. brahmi, "Advanced Power Management and Control Using Fuzzy Backstepping Super-Twisting Controls Designed for Fuel Cell Supercapacitors Hybrid Power Systems for Traction Applications," *J. Control. Autom. Electr. Syst.*, vol. 34, no. 5, pp. 996–1012, Oct. 2023, doi: 10.1007/S40313-023-01014-4/TABLES/6.

 doi:10.20944/preprints202603.1075.v1

46. S. Sharma and V. Kumar, "A Comprehensive Review on Multi-objective Optimization Techniques: Past, Present and Future," *Arch. Comput. Methods Eng.*, vol. 29, no. 7, pp. 5605–5633, Jan. 2022, doi: 10.1007/S11831-022-09778-9.
47. A. El Zerk, M. Ouassaid, and Y. Zidani, "Energy management based fuzzy logic control of hybrid system wind/photovoltaic with batteries," *3rd Renew. Energies, Power Syst. Green Incl. Econ. REPS GIE 2018*, Oct. 2018, doi: 10.1109/REPSGIE.2018.8488819.
48. S. A. Adetoro, L. Olatomiwa, J. Tsado, and S. M. Dauda, "An Overview of Configurations and Dispatch Strategies in Hybrid Energy Systems," *Proc. 2022 IEEE Niger. 4th Int. Conf. Disruptive Technol. Sustain. Dev. NIGERCON 2022*, 2022, doi: 10.1109/NIGERCON54645.2022.9803082.
49. A. B. El-Fawair, K.M. Al-Aubidy, and M. A. Al-Khawaldeh, "Energy Management in Microgrids with Renewable Energy Sources and Energy Storage System," *2023 20th Int. Multi-Conference Syst. Signals Devices, SSD 2023*, pp. 801–806, 2023, doi: 10.1109/SSD58187.2023.10411198.
50. "Energy management in an electrical hybrid system using a fuzzy inference control system | IEEE Conference Publication | IEEE Xplore." Accessed: Sep. 10, 2025. [Online]. Available: https://ieeexplore.ieee.org/document/6761389
51. A. Jain, S. Lalwani, and M. Lalwani, "A Comparative Analysis of MOPSO, NSGA-II, SPEA2 and PESA2 for Multi-Objective Optimal Power Flow," *2nd Int. Conf. Energy, Power Environ. Towar. Smart Technol. ICEPE 2018*, Jul. 2018, doi: 10.1109/EPETSG.2018.8659054.
52. R. Pode, B. Diouf, and G. Pode, "Sustainable rural electrification using rice husk biomass energy: A case study of Cambodia," *Renew. Sustain. Energy Rev.*, vol. 44, pp. 530–542, Apr. 2015, doi: 10.1016/J.RSER.2015.01.018.
53. B. Lwakatare, P. Vyavahare, K. Mehta, and W. Zörner, "Electrification Enhancement Scenarios for Off-Grid Communities in Sub-Saharan Africa-Advancing Energy Access," 2024, doi: 10.20944/preprints202411.0047.v1.
54. Nampower, "SCHEDULE OF THE APPROVED ELECTRICITY TARIFFS FOR THE FINANCIAL YEAR 2025/2026." Accessed: Oct. 31, 2025. [Online]. Available: https://www.nampower.com.na/public/docs/tariffs/NamPower-Distribution-Tariff-Schedule-2025-2026.pdf?